# Study on the Biological Communities and Bioweathering of Marble Surfaces at the Altar of Prayer for Good Harvest in the Temple of Heaven (Beijing, China)

Youping Tian *

School of Earth Sciences and Resources, China University of Geosciences (Beijing), Beijing,China

**Abstract**: This study investigates the biological communities on the marble surfaces of the Altar of Prayer for Good Harvest in the Temple of Heaven, Beijing. The predominant populations are aerial cyanobacteria that thrive in calcareous environments, are drought-resistant, grow slowly, and have strong vitality. These aerial cyanobacteria exhibit different populations compositions depending on the orientation of the marble surfaces. On the east-facing, warm and humid surfaces, the biological communities are mainly composed of small filamentous cyanobacteria such as *Scytonema* sp.2 and coccoid cyanobacteria like *Gomphosphaeria* sp. On the west-facing, hot and humid surfaces, the biological communities are dominated by *Scytonema* sp.1, a small filamentous cyanobacterium, and mosses. On the north-facing, cold and humid surfaces, the biological communities primarily consist of coccoid cyanobacteria such as *Myxosarcina* sp. and *Gomphosphaeria* sp. On the south-facing, hot and dry surfaces, the biological communities are mainly composed of small or large filamentous cyanobacteria like *Scytonema* sp.1 and *Nostoc* sp.. The observed intensity of weathering varies with orientation: south > west > east > north, which is consistent with the weathering patterns observed on the cloud dragon heads in different orientations. The biological communities on the marble surfaces exhibits various colors, with gray-black being the most common, followed by gray-white, black, brown, and dark brown. The gray-black communities are primarily composed of *Myxosarcina* sp. and *Gomphosphaeria* sp.. The biological communities also display different morphologies,

---

\* Corresponding author at: School of Earth Sciences and Resources, China University of Geosciences (Beijing), Beijing,China
E-mail address: typ@cugb.edu.cn (Y. Tian)

including membranous, hairy, carpet-like, leathery, shell-like, and powdery layers. The population composition of these different morphological communities varies. The growth of aerial organisms on the rock surfaces is controlled by both macro-hydrological dynamics and micro-surface topography. On a macro scale, in areas with low rainfall intensity, the biofilm is sparse, and bioweathering is weak. In areas with high rainfall intensity, "ink bands" rich in cyanobacteria form, leading to strong bioweathering. On a micro scale, the micro-topographic features of the rock regulate local hydrological conditions, determining the colonization patterns: rough, uneven surfaces with discrete water films promote point-like biological aggregation, leading to the development of solution pits; linear decorations or joint surfaces with directional water storage drive linear biological expansion, forming solution traces and grooves; smooth, dense surfaces with uniform water film coverage support planar biological growth, ultimately leading to the overall detachment of the weathering layer. The mechanism of bioweathering involves aerial organisms secreting organic acids, which dissolve inorganic salts in the rock, providing nutrients and gradually "eating away" at the rock, destroying its surface structure, and causing progressive weathering. Preventing or reducing the growth of aerial organisms is key to slowing down the bioweathering process of the stone relics at the Altar of Prayer for Good Harvest.

Keywords:Altar of Prayer for Good Harvest, marble, aerial organisms, cyanobacteria, bioweathering

## 1. introduction

The Hall of Prayer for Good Harvest, located in the Temple of Heaven in Beijing, China, was completed in 1420. It served as the site for the emperors of the Ming and Qing dynasties to perform the "Heaven Worship" and "Prayer for Good Harvest" rituals. It is also the largest existing ancient architectural complex for heaven worship in the world. In 1961, the State Council of China designated the Temple of Heaven as a "National Key Cultural Relic Protection Unit." In 1998, it was recognized by UNESCO as a "World Cultural Heritage Site." The hall covers an area of 460 square meters and is built on a three-tiered circular marble platform, which is 6 meters high and surrounded by white stone balustrades. This platform is known as

the Altar of Prayer for Good Harvest (Fig. 1-a). The marble used in the construction is divided into two types: White marble and Bluish-white marble. White marble, due to its fine texture and ease of detailed carving, is often used in decorative parts such as balustrades and carvings. Bluish-white marble, with its higher compressive strength (Ye and Zhang, 2019) and better corrosion resistance compared to White marble (Qu, 2018), is typically used in load-bearing and wear-resistant areas such as the base and paving. Most of the White marble and Bluish-white marble used in the construction come from the marble quarries in Dashiwo Town, Fangshan District, Beijing. (Wu and Liu, 1996; Lü and Wei, 2020). Compared to other types of rock used in the Temple of Heaven complex (such as limestone, granite, and sandstone), the marble used in the Altar of Prayer for Good Harvest is the most susceptible to weathering due to its lower hardness. White marble, a special variety of marble, is particularly sensitive to weathering (Ye and Zhang, 2019). Additionally, because marble is rich in calcium, it serves as a preferred substrate for biological growth (Miller, et al., 2006). However, the organisms are not uniformly distributed across the entire marble surface; their distribution is selective. In addition to requiring a calcium-rich substrate, they also need water. In areas with low rainfall intensity (such as high and protruding locations on the marble surface), where water is scarce, there is little to no biological growth, and the surface appears white or yellowish-white with minimal biofilm and weak bioweathering. In contrast, in areas with high rainfall intensity (such as water convergence points, channels, and Chi Heads), where water is abundant, there is extensive biological growth, and the surface appears black (with patches of brown and gray-black) with a prominent biofilm and strong bioweathering. (Fig.1-b). The gradient distribution of the biofilm on the rock surface is significantly spatially coupled with the variations in instantaneous runoff, reflecting an optimal water allocation mechanism in arid environments (Tian, 2004; Macedo, et al., 2009). In addition to the rock substrate and precipitation, environmental factors such as wind and air pollution also influence microbial colonization, a phenomenon known as "bioreceptivity" of vulnerable structural materials (Guillitte and Dreesen, 1995; Miller, et al., 2012). Among these organisms, cyanobacteria are particularly significant because they can grow with just light and water, and they can survive within the rock, playing a crucial role in the degradation of stone cultural relics (C., Gaylarde, 2020).

a                                                         b

**Fig. 1**. The Altar of Prayer for Good Harvest in the Temple of Heaven, Beijing, China, and the distribution of black biofilm on its marble surface.

a. The three-tiered circular marble platform surrounded by white stone balustrades below the Hall of Prayer for Good Harvest is known as the Altar of Prayer for Good Harvest; b The surface of the Altar of Prayer for Good Harvest marble is covered with black biofilm, which is distributed according to the intensity of rainfall. In areas with low rainfall intensity, the biofilm is not noticeable. In areas with high rainfall intensity (such as channels, water convergence points, and dragon heads), there is a significant distribution of black biofilm.

Black microbial distributions, forming black crusts, have been observed on marble surfaces in many regions (Checcucci, et al., 2022; Monte and Sabbioni, 1986; Praderio, et al., 1993; Gorbushina, et al., 2002). This phenomenon is also referred to as marble blackening (Moropoulou, et al., 1998), bioweathering, or biodeterioration. The microbial communities on marble surfaces exhibit high diversity (Timoncini et al., 2022). The black crust microbial communities are primarily composed of coccoid and filamentous cyanobacteria from the genera *Chroococcus*, *Gloeocapsa*, and *Tolypothrix* (Lombardozzi, et al., 2012), as well as green algae, fungi (Isola, et al., 2016; Leo, et al., 2019; Marvasi, et al., 2012), and lichens (Pinna, et al., 2018). *Chroococcus* can bore into the marble surface, demonstrating remarkable environmental adaptability: not only do they form blue-green biofilms on the rock surface (epilithic growth), but they also penetrate through cracks (chasmoendolithic growth), colonize mineral interstices (cryptoendolithic growth), and even actively excavate (euendolithic growth) deeper into the marble. The tubular tunnels drilled by *Chroococcus* in calcite crystals involve both chemical dissolution and mechanical erosion, making them a dominant species in the community (Golubić, et al., 2015; Scheerer, et al., 2009). Biofilms

alter the thermal and moisture properties of the material, exert colloidal mechanical stress, and secrete acidic and redox metabolites, which intensify mineral lattice destruction and promote the formation of harmful crusts (Guiamet, et al., 2013; Warscheid and Braams, 2000). They can also accelerate rock weathering, leading to the formation of pits (Danin and Caneva, 1990) and control the micro- and macro-morphology of the rock surface (Tian, 2004). Black biofilms on marble surfaces show differential erosion based on orientation, such as differences between windward and leeward faces (Danin and Caneva, 1990). Height differences also play a role, with height having a greater impact on microbial weathering than orientation. The microenvironmental gradients on the rock surface are the core driving factors for the biological erosion of stone cultural heritage (Trovão and Portugal, 2024). In extremely arid environments, "gravel shell" microbial communities composed of lichens, cyanobacteria, and fungi drive the decomposition of rock particles and the formation of primitive soil (terrestrial protopedon) through bioweathering mechanisms such as pH changes, swelling and shrinking, enzymatic activity, and mineral migration (Jung, et al., 2020). Even in areas with fewer black biofilms, the frequency of microbial presence increases as the physical and chemical acid erosion of marble forms a powdery layer, accelerating the transformation of marble into soil and posing a serious threat to marble cultural heritage. Understanding the bioweathering patterns on marble surfaces is crucial for the conservation of marble cultural heritage. For example, targeted use of microbial methods to remove black crusts can be more effective than purely chemical or laser methods (Gioventù, et al., 2011).

Current research on the weathering of marble cultural heritage in Beijing has primarily focused on the roles of physical and inorganic chemical processes, such as acid erosion. Studies have found that the surface peeling and pollution of the marble steles at the Confucian Temple in Beijing are caused by acid rain erosion (He, 2021). Freeze-thaw cycles can lead to internal structural damage in rocks, while salt fog crystallization causes pore expansion and degradation (Li, 2023). Temperature changes affect the physical and mechanical properties of dolomitic marble in Beijing, leading to surface peeling, dissolution of dolomite crystals, and the formation of crusts due to $SO_2$ and dust pollution (Liu, 2020; Zhang, et al., 2016; Wang, et al., 2022). The mechanism of granular peeling on marble surfaces is attributed to the low amount of cementing material between particles, resulting in weak cementation. Surface particles are disrupted by mining unloading, processing damage, stress concentration, and temperature variations, leading to peeling (Wang, 2010).

Temperature fluctuations, acid rain dissolution, water erosion, and salt micro-crack filling are the main causes of weathering in Fangshan marble in Beijing (Zhang, et al., 2015). Research on the weathering of white marble components in the Hall of Supreme Harmony in the Forbidden City indicates that thermal stress from solar radiation and rain erosion are the primary factors (Wu, et al., 2023). It has been found that under the combined action of acid and salt, dolomite crystals degrade through dissolution, interstitial erosion, and spalling. Salt crystallization accelerates the latter two types of damage, while acid erosion promotes salt penetration, significantly increasing the rate of degradation (Zheng, et al., 2025). Regarding bioweathering of marble in Beijing, only a few studies have mentioned it (Beijing Institute of Ancient Architecture, 2018). The main types of damage to marble in Beijing include fissures, peeling, disintegration, crust formation, solution pits, erosion, component loss, discoloration, biological parasitism, and improper human restoration (Yang, 2016). Two types of peeling in white marble in the Beijing area have been identified: one driven by the synergistic effects of thermal weathering, lichen, and rainfall, and the other by acid rain and capillary water absorption (Zhang, 2022). To understand the patterns of bioweathering in marble, it is essential to know the composition, structure, and metabolic potential of the resident microbial communities and their interactions with the stone (Pinna, 2017; Marvasi, et al., 2019). This study focuses on analyzing the community composition, structure, and relative biomass of biofilms on the marble surface of the Altar of Prayer for Good Harvest in Beijing. By identifying the development process and patterns of the biofilm communities, we aim to reveal the mechanisms of biocorrosion and provide a scientific basis for developing more targeted conservation strategies for marble cultural heritage.

1. Overview of the Study Area

Beijing is located in a warm temperate monsoon semi-humid climate zone, characterized by a cool mountain climate. The region has an average annual temperature of 10.8°C, with a frost-free period of approximately 150 days. In winter, Beijing is influenced by cold air masses from the northwest, resulting in a cold and dry climate. The prevailing wind direction during this season is from the northwest, with an average annual wind speed of 1.9 meters per second. In summer, the influence of the subtropical high-pressure system makes the climate hot, and rainfall is relatively

concentrated, especially from July to September, when about 85% of the annual precipitation occurs, often in the form of heavy rain. Autumn in Beijing is generally pleasant, while spring is relatively short. The frost-free period ranges from 190 to 200 days. Under extreme weather conditions, the maximum summer temperature can reach 42°C, and the minimum winter temperature can drop to -25°C. According to data from the National Meteorological Information Center of Beijing from 2009 to 2024, the annual precipitation in Beijing shows significant fluctuations (Fig. 2). There is no clear trend in the annual average relative humidity and annual average precipitation, but there is an increasing trend in the annual average sunshine hours and annual average extreme maximum temperature, and a decreasing trend in the annual average extreme minimum temperature (Fig. 3). During the period from 2009 to 2024, the multi-year average annual total rainfall was 610 mm.
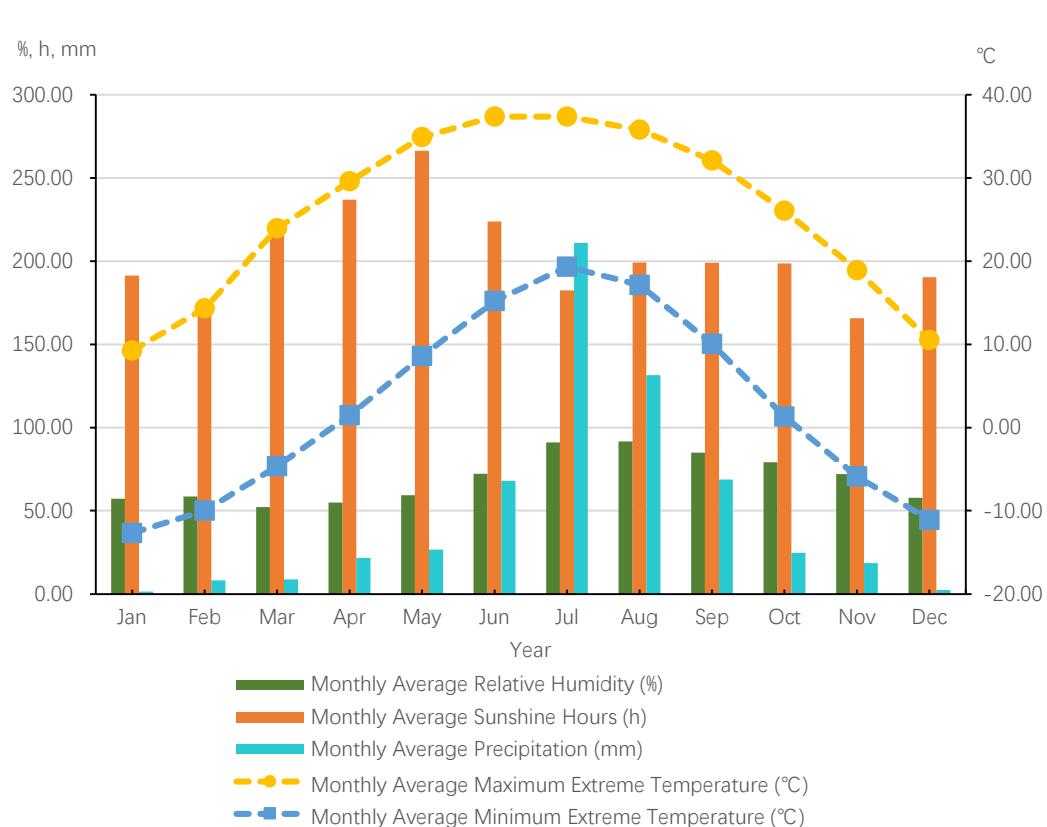
Fig. 2 Monthly average relative humidity, monthly average sunshine hours, monthly average precipitation, monthly average extreme maximum temperature, and monthly average extreme minimum temperature in the Beijing region from 2009 to 2024 (based on data from the National Meteorological Science Data Center Website).

185

191

192

193     The Altar of Prayer for Good Harvests at the Temple of Heaven is a triple-tiered circular altar

194 (Fig. 1-a). Each tier of its white marble base is adorned with 100 intricately carved Chi Heads (Fig.

195 1-b, Fig. 16). The Chi Head (Chi Shou) is a unique functional and decorative architectural element

196 in traditional Chinese architecture, inspired by the mythical hornless dragon-like creature "chi."

197 Resembling a dragon's head without horns, it is commonly found on the roofs, beams, columns, and

198 stone railings of palaces and temples. Its design integrates both aesthetics and practicality: rainwater

199 is channeled through hidden drainage holes in the Chi Heads, preventing water erosion of the base

200 while creating a distinctive visual effect. The three tiers of the altar collectively have a total of 300

201 Chi Heads, with the decorative themes progressively layered—dragon heads (dragon Chi Heads) on

the upper tier symbolize imperial authority, phoenix heads (phoenix Chi Heads) on the middle tier represent auspicious harmony, and cloud patterns (cloud Chi Heads) on the lower tier reflect the connection between heaven and earth. During the rainy season, water cascades from the mouths of the Chi Heads on all three tiers, creating a spectacular sight of "dragons spouting torrents, phoenixes holding pearls, and clouds rolling like waves." Over time, the weathering of the Chi Heads has varied significantly depending on their orientation (Fig. 16), vividly illustrating the dynamic interaction between ancient architectural elements and the natural environment.

The main production area for Beijing marble is Dashiwo Town, located in the southwestern part of Fangshan District, Beijing. In the distribution of marble layers in Fangshan, Bluish-white marble is the first to be quarried due to its shallow burial depth. On the other hand, White marble is found in the deepest layer, with a burial depth that is usually the deepest among the stone layers, ranging from 90 cm to 150 cm in thickness. In the construction industry, both White marble and Bluish-white marble are widely used as marble materials.

## 2 Research Methods

### 2.1 Field Work

Different forms of biofilm communities on the marble surface were collected (biofilms are loose and easily detachable, so a small amount was gently picked by hand without damaging the cultural relics), placed in specimen boxes, numbered, and photographed. The appearance, color, and morphology of the biofilms were described, and the date and location were recorded. The micro-morphologies formed by the dissolution of the biofilm communities were observed and photographed. A total of 40 biofilm community specimens were collected, and 22 photographs of the field biofilm communities were taken. On clear, sunny days, the surface temperature of the rock in the sampling area was measured using an infrared thermometer (DL333380, Deli, China). At the same time, the degree of weathering of the Chi Heads was marked on the overhead view of the Altar of Prayer for Good Harvests. Chi Heads with complete surface ornamentation were marked in green, those with incomplete ornamentation were marked in yellow, and those with completely weathered and disappeared ornamentation were marked in red. Environmental humidity in different directions was measured using a hygrometer (THM-H1, Delixi, China).

232    2.2 Laboratory Work

233    2.2.1 Microscopic Observation

234    The size, morphology, and color of the biofilm communities were observed using a

235 stereomicroscope (Szx7, Olympus, Japan). Then, temporary slides were prepared from different

236 colored biofilm communities and observed under a biological microscope (Bx51, Olympus, Japan).

237 The species of the biofilm communities were identified (Desikachary, 1959; Geitler, 1932; Komarek,

238 1998, 2005, 2013; Zhu, 1991; Fott, 1980; Hu and Wei, 2006), and photographs were taken. For each

239 biofilm community ecological specimen, a microslide was prepared, resulting in a total of 40

240 microslides, and 142 microscopic photographs were taken.

241    2.2.2 Biomass Statistics

242    The volume percentage of the species in the biofilm communities was recorded. The volume

243 percentages of the species were statistically analyzed to calculate the relative volume ($V_x$, relative

244 biomass) and the relative volume percentage ($Y_x$, relative biomass percentage). The statistical and

245 calculation methods are as follows:

246    (1) Relative Volume ($V_x$, Relative Biomass)

247    To obtain the relative volume, the following steps need to be taken:

248    1) Determine the volume percentage ($v(x)\%$)

249    By estimating the percentage of the volume that each species occupies relative to the total

250 volume of all species in each microslide, the volume percentage ($v(x)\%$) of that species in the

251 microslide is obtained. The estimation can be based on the area occupied by each species in the

252 microslide, as within the same microslide, the thickness between the cover slip and the slide is nearly

253 uniform across different areas. Therefore, under the same thickness, the larger the area occupied by

254 a species, the greater its volume (Fig. 4).
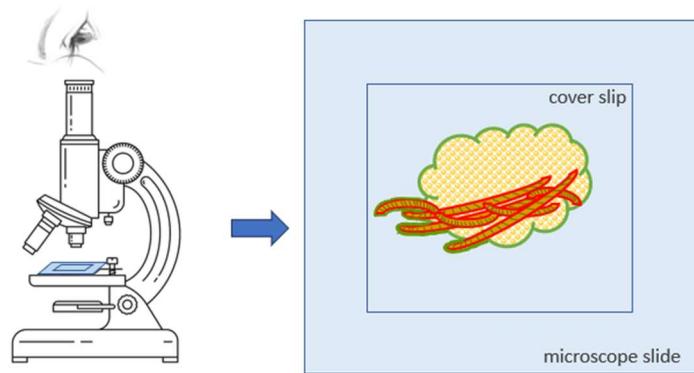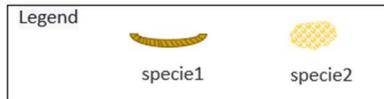
255

256    Fig. 4 Visual Method for the volume percentage (v(x)%) of a Specie

257    in a Biofilm Community Microslide

258    If there are two species in the microslide: Species 1 and Species 2, the volume percentage of Species 1 can be estimated by dividing the

259    area occupied by Species 1 by the total area occupied by both Species 1 and Species 2, and then multiplying by 100. This gives the volume

260    percentage (v(x)%) of Species 1 in the microslide.

261

262    2) Sum the Volume Percentages

263    Add up the volume percentages of the same species across all microslides in the study area to

264    obtain the relative volume (Vx) of a species in the study area. The relative volume of a species

265    roughly reflects its relative biomass in the biofilm community of the study area. It does not represent

266    the actual volume but is an estimated relative value that is meaningful for comparison.

267

268    $$Vx = v(x)_{i_1} + v(x)_{i_2} + \cdots + v(x)_{i_x}$$

269    $i_x$ is the microslide number;x is a specific species(x=a,b,c,…);v(x)$_{ix}$% is the volume percentage of

270    species x.

271    (2) Relative Volume Percentage (Yx, Relative Biomass Percentage)

272    This is the percentage of the relative volume (Vx) of a species in the biofilm community of the

273 study area relative to the sum of the relative volumes of all species in the biofilm community. It is

274 also referred to as the relative biomass percentage.

275

276 $$Y_x = \frac{V_x}{n \times 100} \times 100\%$$

277 n is the total number of microslides.

278

279 The relative volume percentage, also known as the relative biomass percentage, does not

280 represent the actual biomass. This is because it is currently very difficult to accurately measure the

281 biomass of biofilm communities on marble rock surfaces. By estimating through microscopic

282 observation, one can get a rough understanding of the growth status of the biofilm community. It is

283 a relative value and is meaningful only for comparative purposes.

284

285 3 Results

286 3.1 Distribution of communities in the Study Area

287 The composition of the biofilm communities on the marble surface in the study area includes

288 a total of 30 genera and species (Fig. 5). The most abundant species is *Myxosarcina* sp., followed

289 by *Gomphosphaeria* sp., *Asterocapsa* sp., *Gloeocapsa* sp.1 (Fig. 6), and *Scytonema* sp.1, among

290 others.
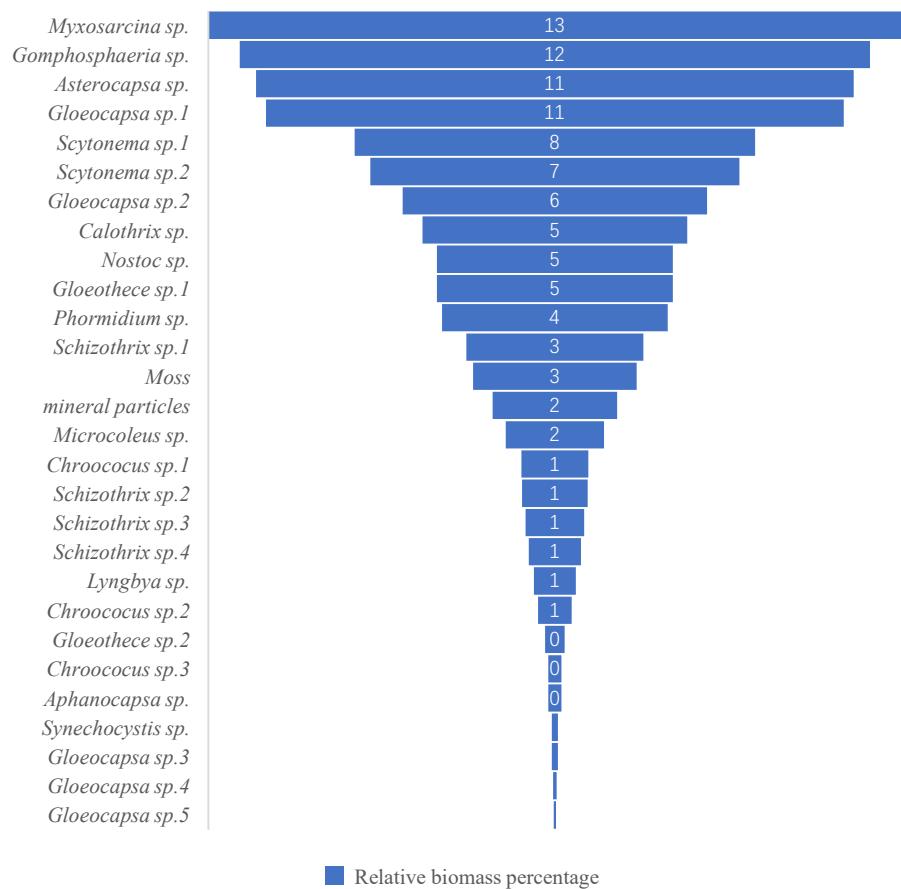
| Species | Relative biomass percentage |
|---|---|
| *Myxosarcina sp.* | 13 |
| *Gomphosphaeria sp.* | 12 |
| *Asterocapsa sp.* | 11 |
| *Gloeocapsa sp.1* | 11 |
| *Scytonema sp.1* | 8 |
| *Scytonema sp.2* | 7 |
| *Gloeocapsa sp.2* | 6 |
| *Calothrix sp.* | 5 |
| *Nostoc sp.* | 5 |
| *Gloeothece sp.1* | 5 |
| *Phormidium sp.* | 4 |
| *Schizothrix sp.1* | 3 |
| *Moss* | 3 |
| *mineral particles* | 2 |
| *Microcoleus sp.* | 2 |
| *Chroococus sp.1* | 1 |
| *Schizothrix sp.2* | 1 |
| *Schizothrix sp.3* | 1 |
| *Schizothrix sp.4* | 1 |
| *Lyngbya sp.* | 1 |
| *Chroococus sp.2* | 1 |
| *Gloeothece sp.2* | 0 |
| *Chroococus sp.3* | 0 |
| *Aphanocapsa sp.* | 0 |
| *Synechocystis sp.* | |
| *Gloeocapsa sp.3* | |
| *Gloeocapsa sp.4* | |
| *Gloeocapsa sp.5* | |

■ Relative biomass percentage

291

294
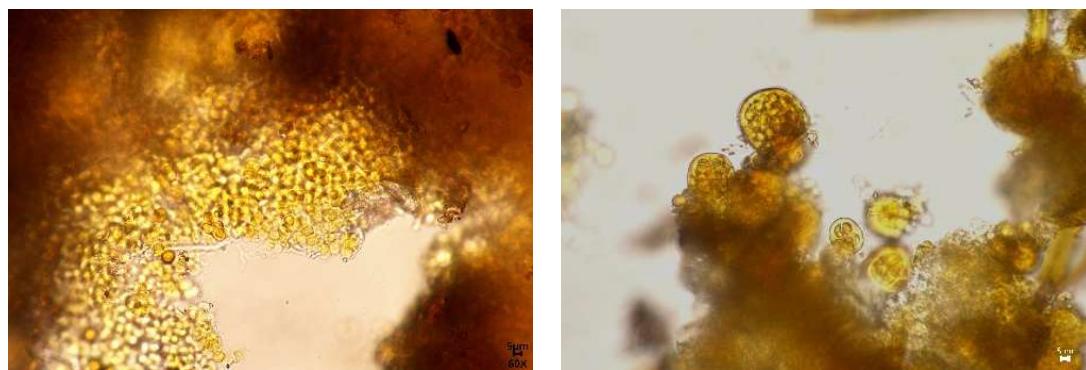
**a.** *Myxosarcina* sp.                  **b.** *Gomphosphaeria* sp.
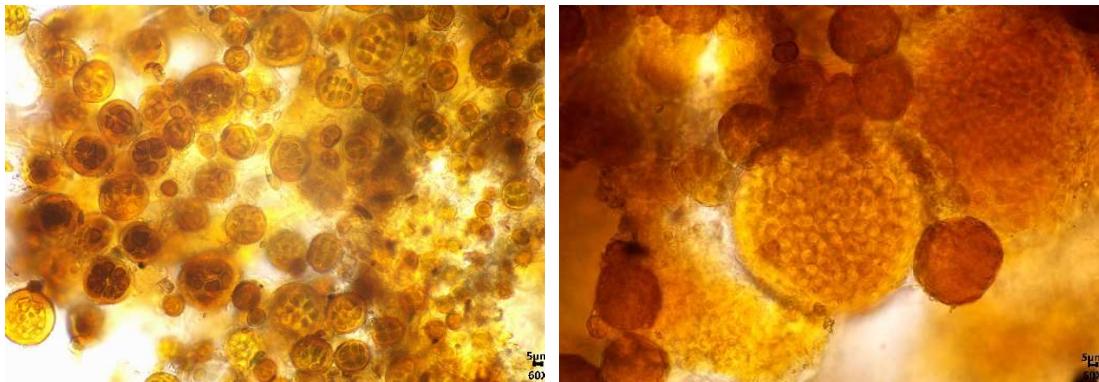
**c.** *Asterocapsa* sp.                 **d.** *Gloeocapsa* sp.1

295 **Fig. 6.** Dominant organisms on the marble surface of the altar of Prayer for Good Harvest

296 in the Temple of Heaven, Beijing., China.

297

298 3.2 Characteristics of the distribution of biological communities on marble surfaces with

299 different orientations in the study area

300 The Altar of Prayer for Good Harvests at the Temple of Heaven is a circular building (Fig. 16).

301 The marble surfaces facing different directions receive varying amounts of sunlight. The south-

302 facing surface receives the most sunlight, followed by the east and west-facing surfaces, which

303 receive sunlight for half a day. The north-facing surface is shaded and receives no direct sunlight.

304 This variation in sunlight exposure leads to differences in the biological populations on the rock

305 surfaces. The details are discussed below:

306

307 3.2.1 Characteristics of Biological communities on East-Facing Rock Surfaces

308 The biological communities on east-facing rock surfaces are primarily characterized by gray-

309 white, gray-brown, brown, gray-black, black-brown, white, and black-brown leathery appearances.

310 The main species include *Scytonema* sp.2, *Chlorococcum* sp., *Gloeocapsa* sp.2, *Gloeothece* sp.1,

311 *Myxosarcina* sp., *Phormidium* sp., *Calothrix* sp., *Gloeothece* sp.2, *Lyngbya* sp., *Gloeocapsa* sp.5,

312 and *Chroococcus* sp.1 (Fig.7) . Among these, the dominant species are *Scytonema* sp.2,

313 *Chlorococcum* sp., accounting for 25% and 23% of the relative biomass percentage(Fig. 8).

314

315
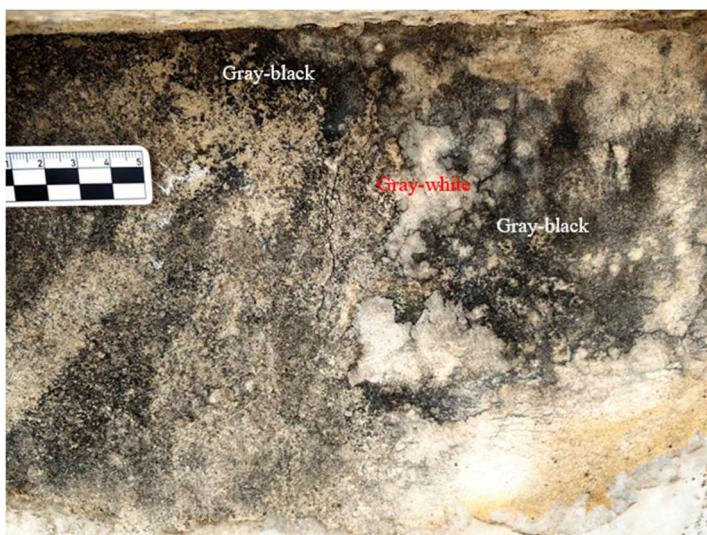
a. Gray-white, Gray-black
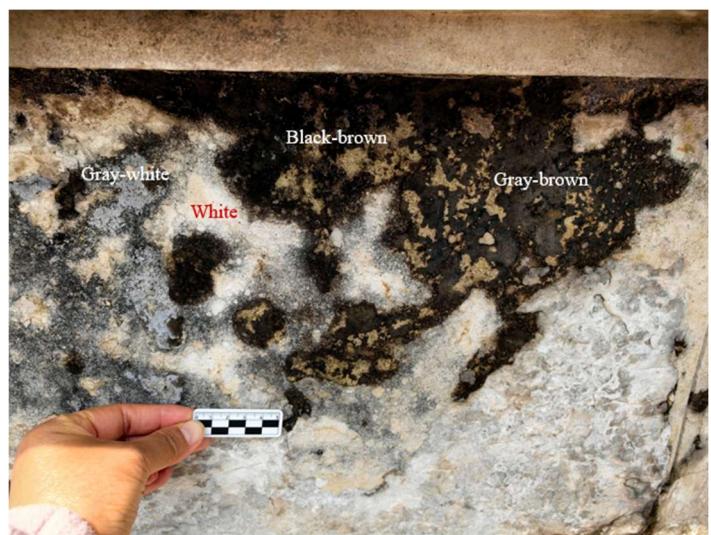
b. Gray-white, Gray-brown, Black-brown, White

c. *Scytonema* sp.2

d. *Gomphosphaeria* sp.

e. *Gloeocapsa* sp.2

f. *Gloeothece sp.1*

316    **Fig. 7.** Micrographs of biological communities and some species on the east-facing marble surface of the altar of

317                Prayer for Good Harvest in the Temple of Heaven, Beijing, China.

| | |
|---|---|
| Scytonema sp.2 | 25 |
| Gomphosphaeria sp. | 23 |
| Gloeocapsa sp.2 | 14 |
| Gloeothece sp.1 | 14 |
| mineral particles | 9 |
| Myxosarcina sp. | 5 |
| Phormidium sp. | 5 |
| Calothrix sp. | 4 |
| Gloeothece sp.2 | 1 |
| Lyngbya sp. | |
| Gloeocapsa sp.4 | |
| Chroococus sp.1 | |

■ Relative biomass percentage

318
319 **Fig.8.** Biological population relative biomass percentage on the east-facing marble surface of the altar of
320 Prayer for Good Harvest in the Temple of Heaven, Beijing, China.

321

322 3.2.2 Characteristics of Biological communities on West-facing Rock Surfaces

323     The biological communities on west-facing rock surfaces are primarily characterized by black
324 hairy, black membranous, yellow-green leathery, gray-black leathery, yellow-green, brown, and
325 gray-green appearances. The main species include *Scytonema* sp.1, mosses, *Schizothrix* sp.1,
326 *Myxosarcina* sp., *Asterocapsa* sp., *Gloeocapsa* sp.1, *Gomphosphaeria* sp., and *Gloeocapsa* sp.2 et
327 al(Fig. 9). Among these, the dominant species are *Scytonema* sp.1 and mosses et al, accounting
328 for 28% and 20% of the relative biomass percentage respectively(Fig. 10).

329

|  |  |
|---|---|
| a. Gray-black leathery | b. Black hairy and membranous |

c. Yellow-green, Gray-green, Brown    d. *Scytonema* sp.1
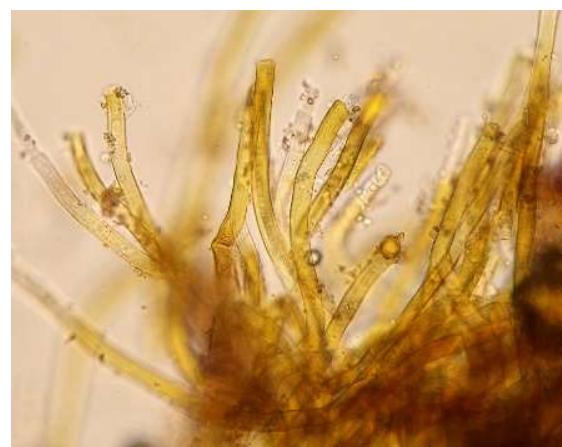
e. moss    f. *Schizothrix* sp.1
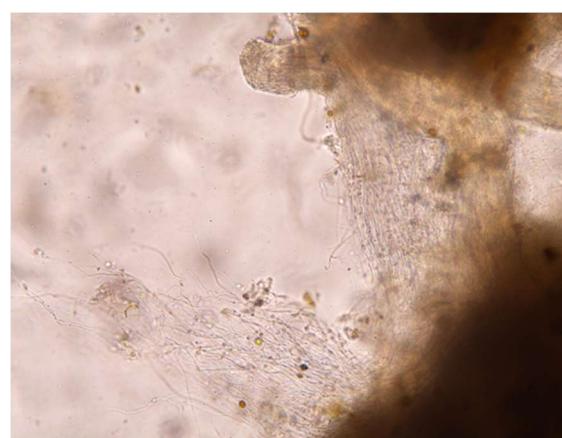
**Fig. 9.** Micrographs of biomes and some species on the west-facing marble surface of the altar of Prayer for Good Harvest in the Temple of Heaven, Beijing, China.

| Species | Relative biomass percentage |
|---|---|
| *Scytonema sp.1* | 28 |
| *Moss* | 20 |
| *Schizothrix sp.1* | 14 |
| *Myxosarcina sp.* | 14 |
| *Asterocapsa sp.* | 10 |
| *Gloeocapsa sp.1* | 6 |
| *Gomphosphaeria sp.* | 4 |
| *Gloeocapsa sp.2* | 4 |
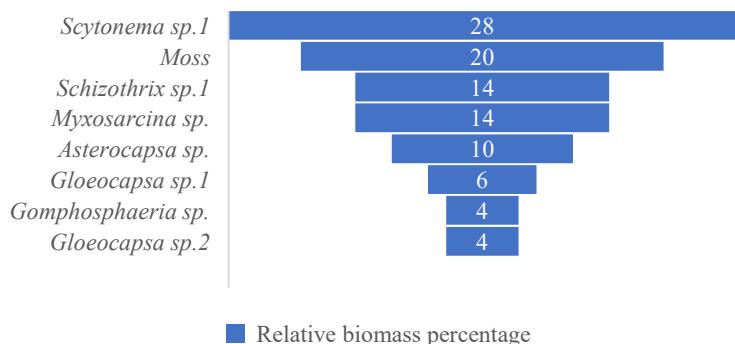
■ Relative biomass percentage

**Fig. 10.** Biological population relative biomass percentage on the west facing marble surface of the altar of Prayer for Good Harvest in the Temple of Heaven, Beijing,China.

337    3.2.3 Characteristics of communities Distribution on North-facing Surfaces

338    The biological communities on north-facing rock surfaces are primarily characterized by gray-

339    brown membranous, brown, gray-black, yellow-green, black-brown, gray-white, brown crusty,

340    brown carpet-like, brown-black leathery, and brown-black membranous appearances. The main

341    species include *Myxosarcina* sp., *Gomphosphaeria* sp., *Gloeocapsa* sp.1, *Schizothrix* sp.1,

342    *Asterocapsa* sp., *Scytonema* sp.1, *Calothrix* sp., mosses, *Gloeocapsa* sp.2, *Microcoleus* sp.,

343    *Chroococcus* sp., *Gloeothece* sp.1, *Lyngbya* sp., *Gloeocapsa* sp., *Scytonema* sp.2, and *Synechocystis*

344    sp. et al(Fig. 11). Among these, the dominant species are *Myxosarcina* sp. and *Gomphosphaeria*

345    sp., accounting for 17% and 15% of the relative biomass percentage respectively(Fig. 12).

346

347

a. Gray-brown membranous                                           b. Gray-black

c. Yellow-green                                                                 d. Gray-white
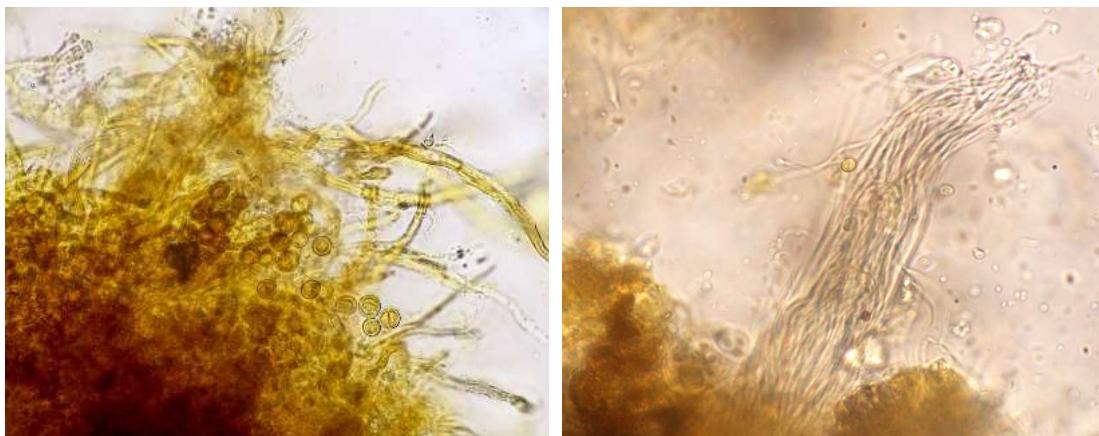
e. *Calothrix* sp.                   f. *Microcoleus* sp.

348   **Fig. 11.** Micrograph of biological communities and some species on the north facing marble surface of the altar of

349   Prayer for Good Harvest in the Temple of Heaven, Beijing, China.

350
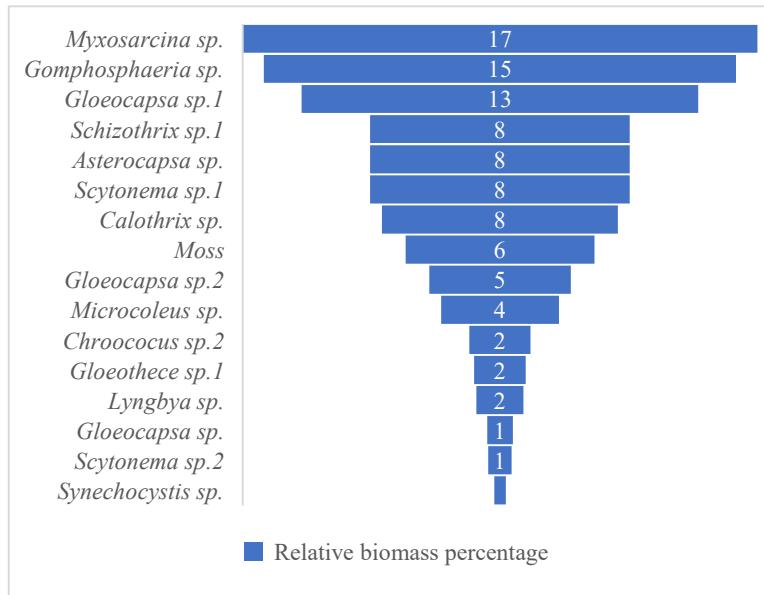
351

352

353   **Fig. 12.** Relative biomass percentage of biological population on the north facing marble surface of the altar of

354   Prayer for Good Harvest in the Temple of Heaven, Beijing,China.

355

356   3.2.4 Characteristics of communities Distribution on South-facing Surfaces

357        The biological communities on south-facing rock surfaces are primarily characterized by gray-

358   green leathery, gray-white, gray-black membranous, black leathery, gray-black, brown-yellow, and

359   green powdery layer appearances. The main species include *Scytonema* sp.1, *Nostoc* sp.,

360    *Asterocapsa* sp., *Myxosarcina* sp., *Phormidium* sp., *Gloeocapsa* sp.1, *Chroococcus* sp.1, *Schizothrix*

361    sp.4, *Microcoleus* sp., *Aphanocapsa* sp., *Chroococcus* sp.3, *Lyngbya* sp., *Gloeocapsa* sp.3, and

362    *Gloeocapsa* sp.4 et al(Fig. 14). Among these, the dominant species are *Scytonema* sp.1 and *Nostoc*

363    sp., accounting for 25% and 20% of the relative biomass percentage respectively(Fig. 15).

a. Some carved decorations have been completely            b. Gray-white, Gray-black

destroyed

c. Black leathery                        d. Green powdery layer

364           **Fig. 13.** Field photo of biomes on the south facing marble surface of the altar of

365                Prayer for Good Harvest in the Temple of Heaven, Beijing, China.

366

367

a. Green powdery layer magnified 60x          b. Green powdery layer magnified 400x
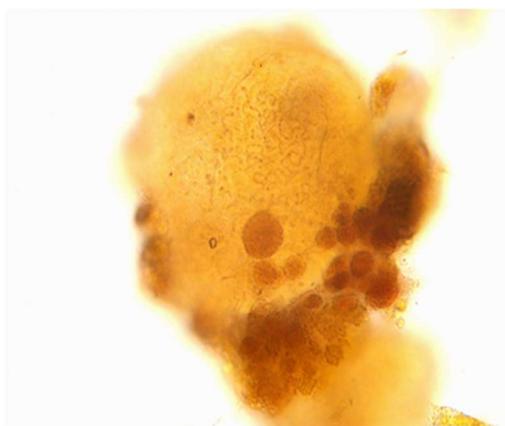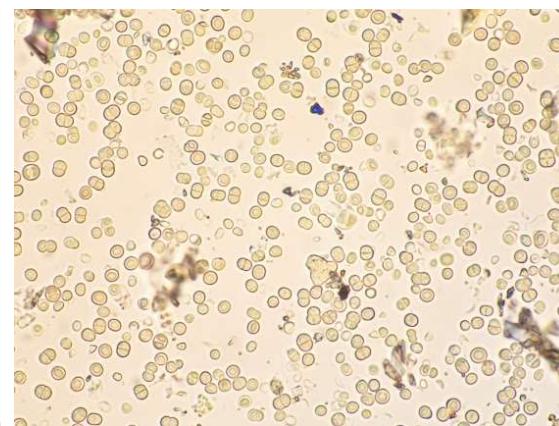
c. *Nostoc* sp.          d. *Chroococus* sp.1
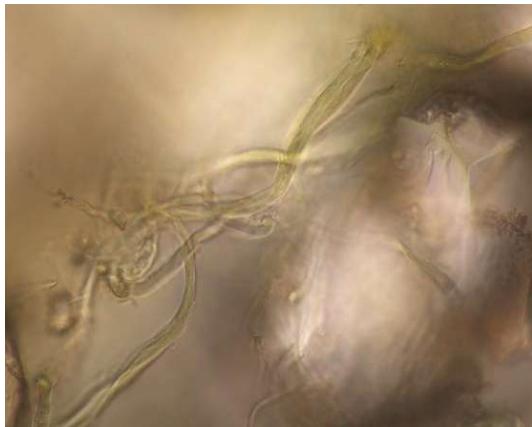
e. *Schizothrix* sp.3          f. *Chroococcus* sp.3
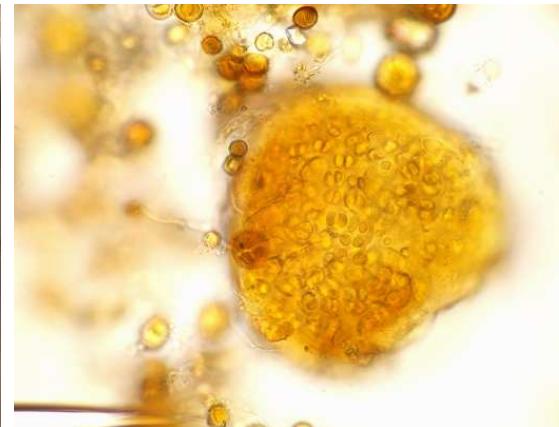
**Fig. 14.** Micrograph of biomes and some species on the south facing marble surface of the altar of Prayer for Good Harvest in the Temple of Heaven, Beijing, China.
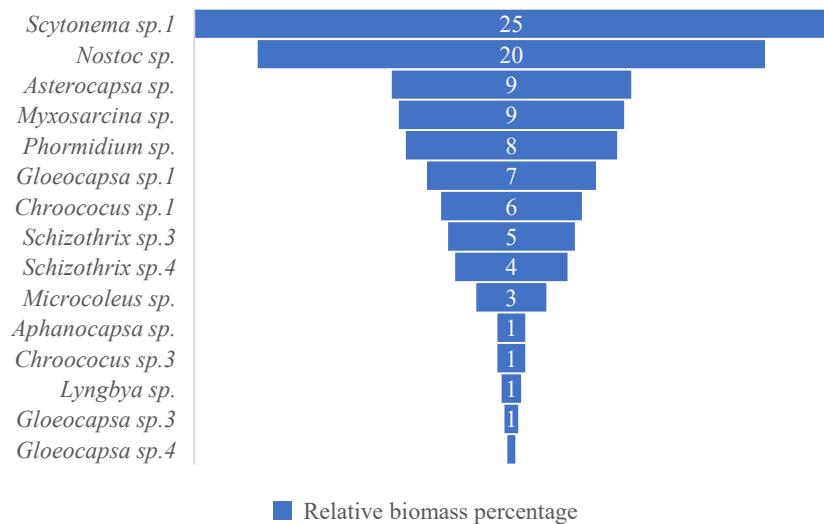
**Fig. 15.** Biological population relative biomass percentage on the south facing marble surface of the altar of

Prayer for Good Harvest in the Temple of Heaven, Beijing, China.

3.2.5 Comparison of communities on Different Orientations

The main aerial organisms on the rock surfaces include spherical cyanobacteria, small filamentous cyanobacteria, and large filamentous cyanobacteria. Their distribution is primarily influenced by the looseness of the substrate, sunlight, and moisture. From spherical cyanobacteria to small filamentous cyanobacteria and then to large filamentous cyanobacteria, the requirement for substrate looseness increases, the need for moisture decreases, and the requirement for sunlight duration increases. Mosses, on the other hand, prefer shady and moist environments.

Although both the east and west-facing surfaces of the Altar of Prayer for Good Harvests in the Temple of Heaven receive sunlight for half a day (Table 1), the east-facing surface receives sunlight in the morning when the rock surface temperature is lower. Even with sufficient sunlight, the growth of organisms on the east-facing surface is not as robust as on the west-facing surface. The west-facing surface receives sunlight in the afternoon when the rock surface temperature is higher, providing both water and heat conditions that are more favorable for biological growth. This results in the presence of *Scytonema* sp.1, a cyanobacterium that prefers looser substrates, and more mosses, leading to more severe weathering on the west-facing surface. The north-facing surface, being in the shade, has slower evaporation rates and is mainly colonized by spherical cyanobacteria,

resulting in relatively weaker weathering. The south-facing surface receives more sunlight and weathers faster, with the carved decorations on the rock surface completely destroyed (Fig. 13a). The matrix is highly loose, and even large filamentous cyanobacteria like *Nostoc*, which typically prefer to live in soil rather than on rock surfaces, are present. This indicates that the south-facing marble has weathered severely, forming a loose, soil-like thick weathering layer. Additionally, *Scytonema* sp.1, a species that thrives in sunny and dry environments and plays a significant role in bioweathering, is also present. Mosses are not found on the south-facing side because they prefer shady and moist environments. The orientation of the building, through differences in sunlight duration and evaporation rates, creates a unique gradient of microhabitats, which in turn drives the differential distribution of microbial communities and is accompanied by varying degrees of weathering depending on the direction.

To further understand the environmental differences and weathering conditions of the rock surfaces at the Altar of Prayer for Good Harvests in the Temple of Heaven, temperature measurements were taken on a sunny afternoon in April (Fig. 16). The rock surface temperatures were found to be highest in the southwest and lowest in the northwest. The Altar of Prayer for Good Harvests was divided into four natural sectors, each centered on a cardinal direction and covering 45° to either side: North (N): 315°-45°, centered on true north, covering from northwest to northeast; East (E): 45°-135°, centered on true east, covering from northeast to southeast; South (S): 135°-225°, centered on true south, covering from southeast to southwest; West (W): 225°-315°, centered on true west, covering from southwest to northwest. The weathering degree of 100 cloud dragon heads on the third layer was statistically analyzed in each sector. The results showed that 40% of the south-facing cloud dragon head decorations were completely weathered, indicating the most severe weathering. The weathering degrees for the west, east, and north sectors decreased in that order. This pattern is consistent with the distribution of biological organisms on the rock surfaces, as shown in Table 1. The analysis of the weathering degree of 100 cloud dragon heads on the third layer showed that 40% of the south-facing cloud dragon head decorations were completely weathered, indicating the most severe weathering. The weathering degrees for the west, east, and north directions decreased in that order. This pattern is consistent with the differences in weathering in different directions revealed by the distribution of biological organisms on the rock surfaces (Table 1).

423
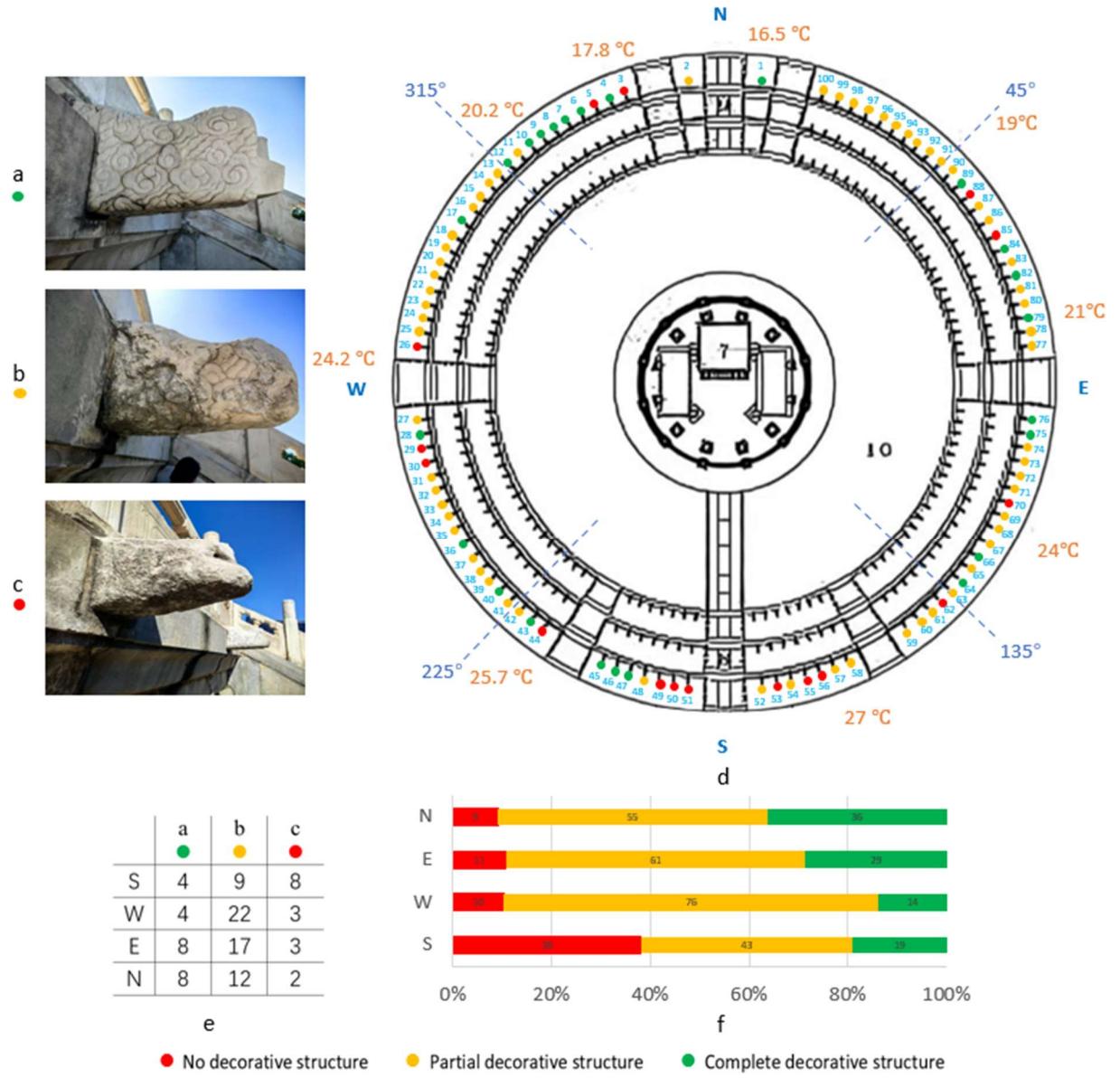
Fig. 16 Rock surface temperatures and weathering conditions of the cloud dragon heads on the third layer of

the Altar of Prayer for Good Harvests at the Temple of Heaven in Beijing, China, on a sunny afternoon in April.

a: Cloud dragon heads with complete decorative structures.

b: Cloud dragon heads with partially weathered decorative structures.

c: Cloud dragon heads with completely weathered decorative structures.

d: A top-down simplified diagram of the Altar of Prayer for Good Harvests. The altar is divided into three layers, with 100 dragon

heads arranged along the edge of each layer. The dragon heads exhibit different degrees of weathering: red indicates completely weathered

decorative structures, yellow indicates partially weathered decorative structures, and green indicates intact decorative structures.

e: Statistical count of the number of cloud dragon heads with three different weathering degrees in four directions.

f: Calculation of the proportion of the three different weathering degrees of cloud dragon heads in different directions, revealing that

434      the weathering intensity of the dragon heads is highest in the south, followed by the west, east, and north.

435

436      **Table 1**

437      Environmental characteristics and dominant species of marble surface of the Altar of Prayer for Good

438      Harvests at the Temple of Heaven in Beijing, China.

439

| Marble Surface Orientation | Sunlight | Moisture | Environmental Characteristics | Dominant Species | Weathering degree |
|---|---|---|---|---|---|
| North-facing | None | Slow evaporation | Cold and humid | Spherical cyanobacteria | |
| East-facing | Half day | Rapid evaporation in the morning | Warm and humid | Small filamentous cyanobacteria, Spherical cyanobacteria | Weak ↓ |
| West-facing | Half day | Rapid evaporation in the afternoon | Hot and humid | Small filamentous cyanobacteria, Mosses | |
| South-facing | Full day | Rapid evaporation during the day | Hot and dry | Small filamentous cyanobacteria, Large filamentous cyanobacteria | Strong ↓ |

440

441 **3.3** Relative Biomass of Different Colored Biological Communities on Rock Surfaces in the Study

442 Area

443      The colors displayed by organisms on rock surfaces differ from those observed under a

444 microscope. In this paper, the former is referred to as the "visual color," while the latter is called the

445 "microscopic color." The visual color is the community color presented when different populations

446 aggregate together, whereas the microscopic color is the color of different species observed under

447 magnification through a microscope. Often, communities of cyanobacteria with different

448 microscopic colors appear mostly black or gray-black of visual color.

449      The visual colors of biological communities on rock surfaces in the study area can be

450 categorized into gray-black, gray-white, black, brown, black-brown, gray-brown, yellow-green,

451 gray-green, white, green, and brown-yellow. Their relative biomass is shown (Fig. 17) . The most

452 common color is gray-black, followed by gray-white, black, brown, and black-brown. These are

453 also typical colors exhibited by aerial cyanobacteria in the field, sometimes referred to as "ink

454 bands." For example, the Nine Horses Fresco Hill (Jiuma Huashan) in the Guilin landscape of China

455 is formed due to aerial cyanobacteria growing on the rocks, creating black ink-like bands.
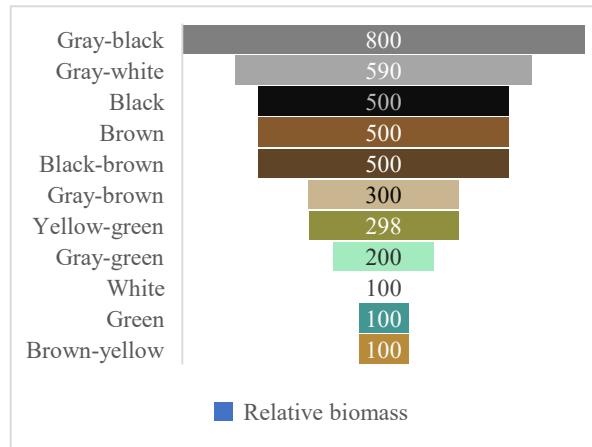
456

457 **Fig. 17** Relative biomass of biomes with different colors on the marble surface of the Altar of Prayer for Good

458 Harvests at the Temple of Heaven in Beijing, China.

459

460 3.4 Relative biomass of communities' composition in different colored biological communities on

461 rock surfaces in the study area

462 The relative biomass of different visual color biotic communities on the rock surface in the

463 study area is shown (Fig. 18). An analysis of the main population compositions of these biological

464 communities is presented (Fig. 19). The colors of biological communities on rock surfaces in the

465 study area are primarily composed of black, brown, gray, green, and yellow, as well as combinations

466 of these colors (gray-black, gray-white, black-brown, gray-brown, yellow-green, gray-green, and

467 brown-yellow). The correlation between color combinations and population composition is not very

468 apparent, which also indicates that determining microscopic color (population composition) through

469 visual color is a complex and difficult task. Nevertheless, some patterns can be observed: Species

470 like *Scytonema* sp.1, *Myxosarcina* sp., *Asterocapsa* sp., *Gomphosphaeria* sp., and *Gloeocapsa* sp.2

471 tend to make the community color darker, presenting as black, brown, gray, or combinations of these;

472 The parts that have a visual color of white are minerals, not biological organisms, under microscopic

473 observation; the areas with a visual color of green (mainly referring to the characteristic blue-green

474 of cyanobacteria) are mineral particles and *Chroococcus* sp.1; the areas with a visual color of

475 yellow-green are mainly mosses; the areas with a visual color of brown-yellow are mainly *Nostoc*

476 sp. etc.

477
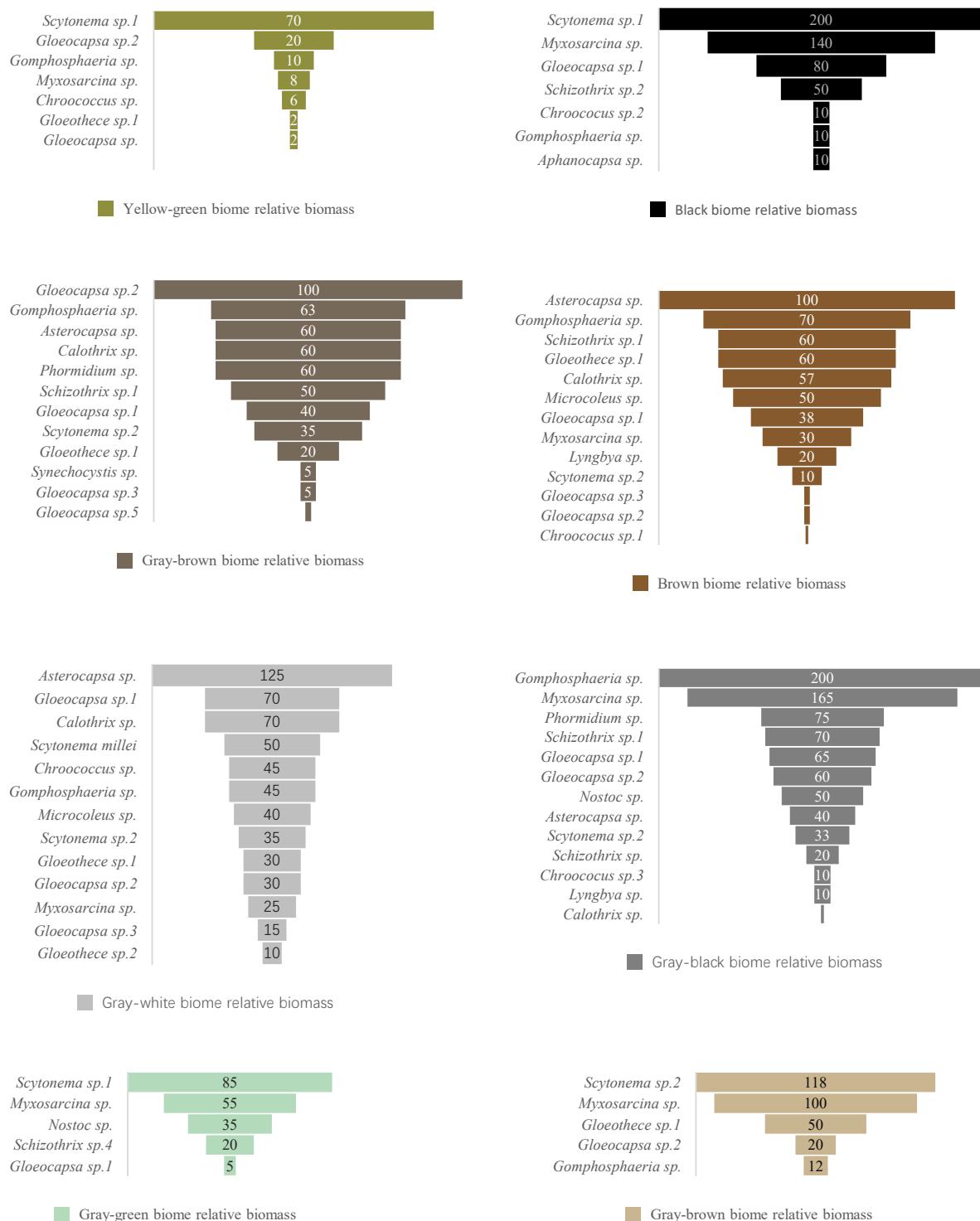
**Fig. 18.** Relative biomass of community composition of different colors on marble surface of the Altar of Prayer for Good Harvests at the Temple of Heaven in Beijing, China.
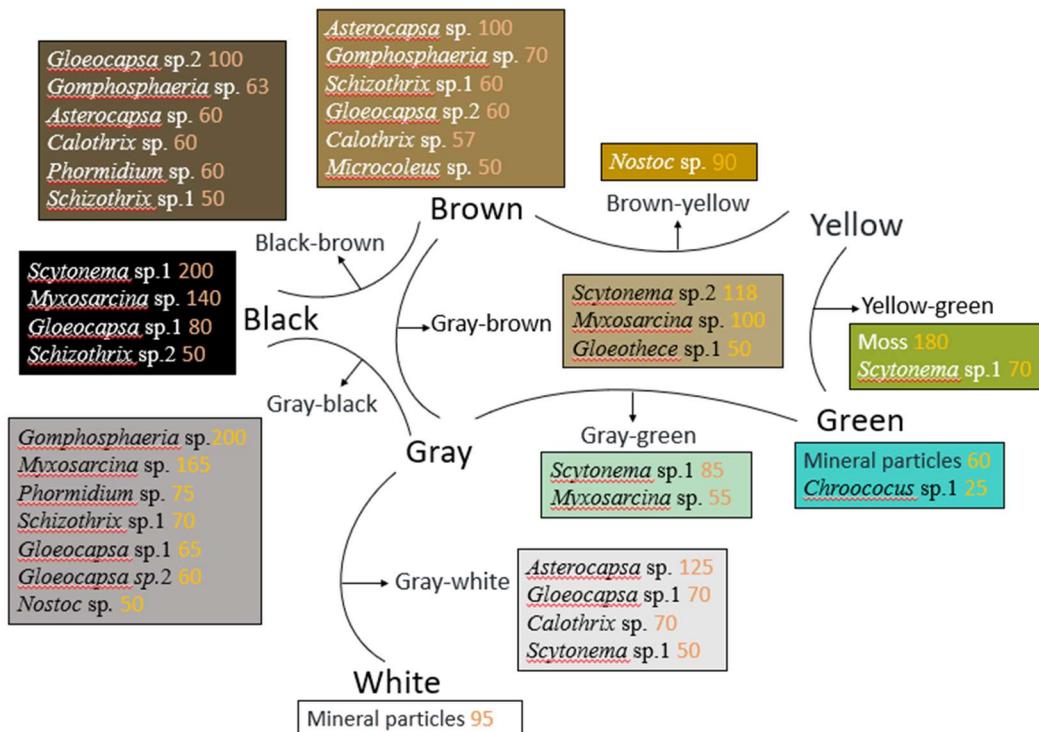
**Fig. 19.** Analysis of main population composition of different color biomes on marble surface of the Altar of Prayer for Good Harvests at the Temple of Heaven in Beijing, China.

3.5 Relative biomass of communities composition in different morphological biological communities on rock surfaces in the study area

The biological communities on rock surfaces in the study area exhibit different morphologies, including membranous, hairy, carpet-like, leathery, shell-like, and powdery layers. Their relative

489    biomass of population composition is shown (Fig. 20). A diagrammatic explanation of the formation

490    of these community morphologies is presented (Fig. 21).
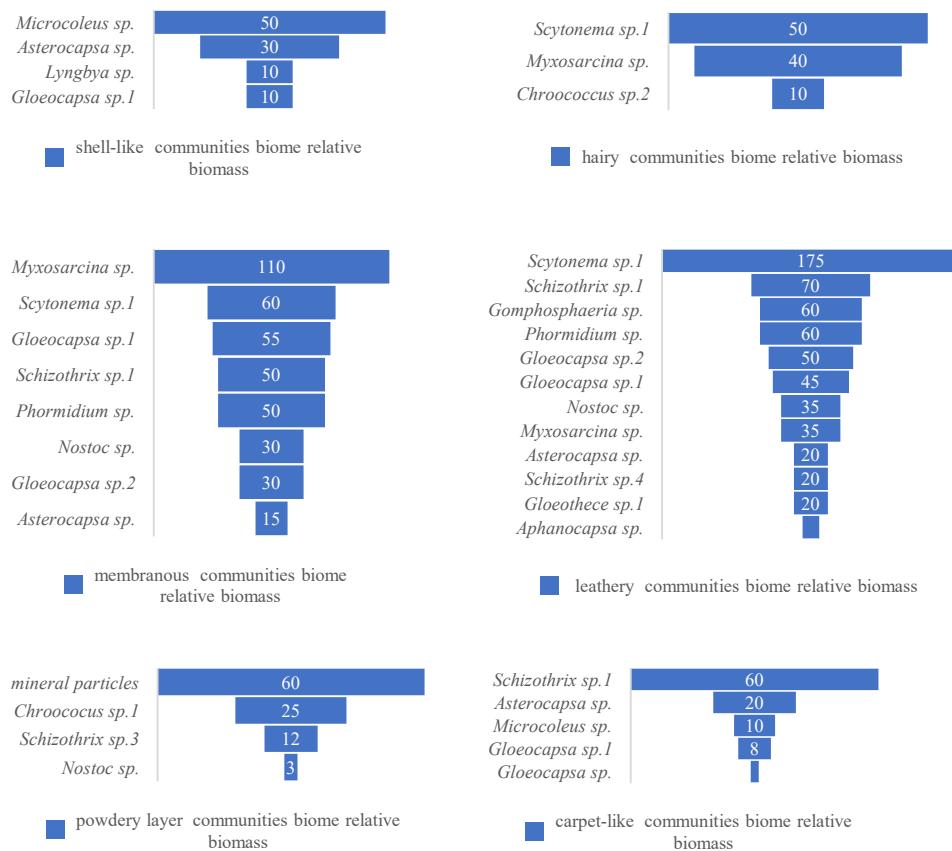
491    **Fig. 20.** Relative biomass of different forms of community on marble surface of the Altar of Prayer for Good

492    Harvests at the Temple of Heaven in Beijing, China.

493

494

495 **Fig. 21** Morphological genesis diagram of different communities on marble surface of the Altar of Prayer for Good

496 Harvests at the Temple of Heaven in Beijing, China.

497

498     The dominant species in the membranous biological communities are mainly *Myxosarcina* sp.

499 and *Scytonema* sp.1. The former accounts for a relative biomass of 110, while the latter accounts for

500 60(Fig. 17). *Myxosarcina* sp. is spherical cyanobacteria (Fig.4a). It has thick individual sheaths,

501 forming a dense colonial mucilage. *Scytonema* sp.1 grows interspersed within, forming a

502 membrane-like community (Fig.21). When the relative biomass of *Scytonema* sp.1 in the

503 community exceeds that of *Myxosarcina* sp., it forms a hairy community (Fig.21). The dominant

504 species in the carpet-like communities are mainly *Schizothrix* sp.1 and *Asterocapsa* sp.. The former

505 accounts for a relative biomass of 60, while the latter accounts for 20 (Fig.20). *Schizothrix* sp.1

506 grows densely together, forming a carpet-like structure (Fig. 21). The dominant species in the

507 leathery biological communities are mainly *Scytonema* sp.1 and *Schizothrix* sp.1. The former

508 accounts for a relative biomass of 175, while the latter accounts for 70 (Fig. 20). *Scytonema* sp.1

509 intertwines, with *Schizothrix* sp.1 interspersed within (Fig. 21). The dominant species in the shell-

510 like biological communities are mainly *Microcoleus* sp. and *Asterocapsa* sp.. The former accounts

511 for a relative biomass of 50, while the latter accounts for 30 (Fig.20). *Microcoleus* sp. has well-

512 developed sheaths, with multiple algal filaments inside each sheath. The sheaths of multiple

513 *Microcoleus* sp. aggregate to form a mucilaginous layer, with *Asterocapsa* sp.1 dispersed within.

514 When the mucilaginous layer dries, it cracks into numerous small pieces. The edges of each piece

515 detach from the rock surface and curl up, forming a shell-like structure(Fig. 21 and Fig. 22). The

516 powder layer is a severely weathered surface (Fig. 13d). Under microscopic observation, it mainly

517 consists of mineral particles and *Chroococus* sp.1, with the former accounting for 60 and the latter

518 for 20 of the relative quantity (Fig. 20). *Chroococus* sp.1 is distributed on the surface and in the

519 crevices of mineral particles (Fig. 14a and b). The color of the community appears as a mixture of

520 the green color of *Chroococus* sp.1 (or the blue-green color characteristic of cyanobacteria) and the

521 white color of mineral particles.

522

523    3.6 Bioweathering on Rock Surfaces in the Study Area

524    The growth distribution of aerial organisms on rock surfaces in the study area is closely related

525 to the surface smoothness and texture of marble (Table 2). If the marble surface is uneven or has a

526 non-uniform texture, the aerial organisms' communities will be distributed in a spotted pattern (Fig.

527 22a). Dissolution forms solution pits and cavities (Fig. 22b), which further expand into solution

528 basins (Fig. 22c, d). If the marble surface has linear textures or non-uniform texture with joint stripes,

529 the aerial organisms' communities will be distributed in a linear pattern (Fig. 22e). Dissolution forms

530 solution marks and grooves (Fig.22f), which further expand into solution channels (Fig. 22g). If the

531 marble surface is smooth and has a uniform texture, the aerial organisms' communities will be

532 distributed in a planar pattern (Fig. 22h). Dissolution forms a weathering layer or spalling layer (Fig.

533 22i).

534

535    **Table 2**

536    Characteristics of the Marble Surface of the Altar of Prayer for Good Harvests in the Temple of

537    Heaven, Beijing, China, and the Process of Biological Erosion on Its Surface.

| Marble Characteristics | Biological Community Distribution | Resulting Dissolution Forms | Development Process |
|---|---|---|---|
| Uneven surface or non-uniform texture | Spotted distribution | Solution pits, cavities, and basins | |
| Surface with linear textures or non-uniform texture with joint stripes | Linear distribution | Solution marks, grooves, and channels | ↓ |
| Smooth surface with uniform texture | Areal distribution | Weathering layer, spalling layer | |

538

539

540

541

a. biological community point distribution      b. Solution pores and solution cavities      c. Sinkhole

d. Solution pit

e. biological community linear distribution

f. Solution marks and solution grooves

g. Solution channel

h. biological community areal distribution

i. Spalling layer

**Fig. 22** Bioweathering forms on the marble surface of the Altar of Prayer for Good Harvests in the Temple of Heaven, Beijing, China.

The spotted distribution of biological communities gradually expands into linear distribution, and then into areal distribution. Solution pits, basins, and cavities also further enlarge their dissolution forms, developing into solution marks, grooves, and channels. For example, in the study

549    area, the weathering process of white marble "cloud Chi Head" begins with the accumulation and

550    growth of organisms in the low-lying areas of the cloud patterns (Figures 23a, b).. These areas retain

551    more moisture, so they are the first to undergo bioweathering, forming deeper solution cavities and

552    channels. The communities then gradually spread to the surrounding areas, developing into linear

553    distributions, and then areal distributions, leading to flaking of the rock surface (Fig. 23c). This

554    partially destroys the pattern structure, further expanding the area and depth of dissolution, forming

555    a loose powder layer (Fig. 13a, d; Fig. 14a, b; Fig. 16b, c; Fig. 23d, e).

556

a. The organisms gather and grow in the low-lying areas of the cloud chi head ornamentation.

b. The organisms gather and grow in the low-lying areas of the cloud chi head ornamentation.

c. The surface of the cloud chi head is flaking off in patches.

d. The cloud chi heads have even weathered away completely.

e. A loose, powdery layer has formed on the surface of the cloud chi heads, with a large amount of cyanobacteria growing inside.

557    **Fig. 23.** Bioweathering process of the cloud Chi Head on the Altar of Prayer for Good Harvests in the Temple of

558                        Heaven, Beijing,China.

559

## 4 Discussion

(1) This study focuses on the cyanobacterial and bryophyte communities that can be observed using biological microscopy. The current scope of the research has not yet covered other microbial groups. To determine whether other bacterial groups exist on the surface of stone cultural relics and to understand their ecological functions, further systematic verification through subsequent studies is still needed. At the methodological level for the classification and identification of cyanobacteria, traditional morphological identification, although it may lead to taxonomic deviations at the genus and species levels, molecular biology methods also face technical bottlenecks. For special samples like biofilms on stone cultural relics, molecular testing typically requires microbial samples with a high purity of more than 0.2 grams. However, in actual sampling, due to restrictions on cultural relic protection, sometimes only trace amounts of less than 0.01 grams can be obtained. While such low sample quantities are sufficient for morphological identification under a biological microscope, they pose significant challenges for molecular biology methods. Low DNA extraction efficiency and significant amplification bias from such small samples can result in decreased taxonomic resolution. Furthermore, there has been long-standing controversy in the taxonomy of cyanobacteria. The conflict between traditional morphological classification and molecular systematics has led to a dynamic revision of the taxonomic framework. This instability makes it difficult to match taxonomic information when annotating environmental samples using 16S rRNA gene sequence databases (Lefler, et al., 2023). Future research should aim to construct a multidimensional identification system, integrating microscopic observation, culturomics, and metagenomics, to gradually establish classification standards and databases suitable for the study of microorganisms in cultural heritage. This will be an important direction for the development of methodologies in this field.

(2) The differential weathering characteristics of the cloud chi heads on the Altar of Prayer for Good Harvests, as well as the directional differences in the spatial distribution of organisms on the rock surface, show significant consistency. This correspondence confirms the scientific validity of the visual analysis method based on the relative volume and the relative volume percentage determined by microscopic observation. This method, through the analysis of micro-scale biotic community features, can effectively reflect the differences in weathering processes in the macro-

(4) The connections and issues between different research levels, methods, and results in this

paper.

Connections and issues between different research levels, methods, and results in this paper.

This paper studies the aerial organisms on rock surfaces in the research area in terms of biological

community population composition, community color and morphology, and community distribution

characteristics (Table 3). The spotted, linear, and planar distributions of biological communities on

rock surfaces in the study area are composed of many microcommunities. These microcommunities

exhibit different morphologies, including membranous, hairy, carpet-like, leathery, shell-like, and

618 powder layers. Spotted, linear, and areal distributions of biological communities may be composed

619 of one type of microcommunity or multiple types. Microcommunities are further composed of

620 multiple populations, and a population consists of multiple individual organisms of the same species.

621 Community distribution characteristics are observed with the naked eye, without

622 magnification. Community color and shape are observed through stereomicroscopes and the naked

623 eye, magnifying objects 8-56 times (or no magnification if observed with the naked eye). Biological

624 community population composition is identified through biological microscope observation,

625 magnifying objects 40-1000 times. This represents three stages of research with increasing

626 magnification of the research object: 1) Distribution area; 2) Community; 3) Population. Research

627 at each stage is relatively easy to conduct, but the connections between stages are challenging and

628 represent a key focus of this paper. For example, to accurately correlate different colored and shaped

629 communities with their precise population compositions (i.e., connecting the community stage with

630 the population stage) requires statistical analysis of numerous specimens to improve accuracy.

631 Additionally, for outdoor observations of communities, which involve the transition between the

632 distribution area stage and the community stage, the primary method is still visual observation with

633 the naked eye. Only a small number of observations are conducted using stereomicroscopes because

634 detailed stereomicroscopic observations that require photography must be done indoors. Sampling

635 of cultural relics in scenic areas is extremely limited and must be carried out without damaging the

636 relics. To address this issue, one approach is to enhance the performance of observation equipment

637 to allow for in situ biological community observations outdoors without sampling, or to perform

638 minimal sampling.

639 **Table 3**

640 Analysis of Research Levels in the Study on aerial organisms on marble of the Altar of Prayer for Good Harvests

641 in the Temple of Heaven, Beijing, China.

| Research Level | Distribution Area | Community | Population |
|---|---|---|---|
| Observation Method | Naked eye | Stereomicroscope, naked eye | Biological microscope |
| Magnification | 0 | 8-56, 0 | 40-1000 |
| Classification | 3 distribution characteristics (point, linear, and areal | 11 colors: | 30 genera and species : |

| | | | |
|---|---|---|---|
| distribution) | | gray-black, gray-white, black, brown, black-brown, gray-brown, yellow-green, gray-green, white, green, brown-yellow | *Myxosarcina* sp.,*Gomphosphaeria* sp.,*Asterocapsa* sp. and so on (Fig.5) |
| | | 6 morphologies: membranous, hairy, carpet-like, leathery, shell-like, and powder layer | |
| Composition | Composed of multiple communities | Composed of multiple populations | Composed of multiple individuals of a single species |

642

(5) In this study, the weathering intensity of the Altar of Prayer for Good Harvests in the Temple of Heaven is found to be south-facing > west-facing > east-facing > north-facing. Additionally, the metabolic activity of the southeastern microbial community on the marble of Florence Cathedral is higher than that of the northwestern community (Checcucci, et al., 2022). This indicates that the weathering of stone cultural relics exhibits directional differences, and these directional differences vary in different climate zones. When studying the microenvironment of rock surfaces, temperature is relatively easy to measure, but humidity is difficult to measure accurately due to the significant influence of wind disturbances, which can lead to measurement failures. Therefore, more effective methods are needed to address this issue. Another comparison can be made between the marble relics of the Cathedral of Santa Maria del Fiore in Florence, Italy, and the Speranza statue (the Cathedral of Santa Maria del Fiore was completed in 1887 and is 135 years old; the Speranza statue was built in 1863 and is 158 years old). The growth of black biofilm on these structures is significantly more extensive and faster than that on the Altar of Prayer for Good Harvests at the Temple of Heaven in Beijing (built in 1420 and 605 years old). The primary reason for this difference is the climate. Florence has a Mediterranean climate with high rainfall (about 850 mm) (Venturi et al., 2020), while Beijing has a temperate monsoon climate with low annual rainfall (During the period from 2009 to 2024, the multi-year average annual total rainfall was 610 mm,

a          b

c

with a small area covered by black biofilm, mainly distributed in areas with high runoff from sudden rain.

(6) The species in the study area, such as *Scytonema* sp.2, are also common aerial cyanobacteria found on limestone surfaces (Tian, et al., 2002; Tian, et al., 2003; Tian, et al., 2004). They prefer calcareous environments, are drought-resistant, grow slowly, and have extremely strong vitality. The mechanism of dissolve rocks primarily involves the biological need to obtain inorganic nutrients such as calcium and magnesium ions from the rock. Aerial organisms can secrete organic acids, which release calcium and magnesium ions from the rock, providing the inorganic nutrients necessary for their growth and development. Through this acid dissolution process, aerial organisms can "eat away" at the rock, forming small hemispherical dissolution pits. This process damages the surface structure of the rock, leading to the formation of an underlying weathering layer (Tian, et al., 2004). In addition, various forms of cyanobacterial communities in extremely arid environments, such as on rocks, develop thicker exopolysaccharide (EPS) sheaths to retain intracellular water. The EPS sheath undergoes contraction and expansion in response to changes in weather conditions, accelerating the disintegration of rock particles on the surface of rocks. This process is very similar to microbial weathering in the Atacama Desert (Jung, et al., 2020). Both processes involve the swelling of the EPS due to water absorption, leading to the deformation of the biofilm and the detachment of the rock surface at the community scale. This results in the expansion of patchy weathering into a more extensive weathering layer (such as the Atacama terrestrial protopedon or the powdery layer at the Temple of Heaven) at the landscape scale. The mechanism involves the tensile stress generated by the swelling of the EPS exceeding the local tensile strength of the rock, initiating cracks (such as grain boundary cracking in the Atacama and mineral particle detachment at the Temple of Heaven). These cracks provide pathways for chemical and biological erosion, leading to an expanded pore/crack network, increased water retention time, enhanced biological activity, and further swelling, creating a self-reinforcing weathering loop. It is clear that the swelling effect plays a crucial role as a "physical engine" in microbial bioweathering. Future research should focus on cross-scale mechanical modeling: scaling up the swelling force of microbial EPS (at the nN level) to the point of rock fracture (at the MPa level) to reveal the mechanisms of scale transition; quantifying the impact of changes in fog/rain patterns under global warming on the frequency of biological swelling, to warn of accelerated weathering risks; and recognizing that swelling not only acts as a "trigger" for rock destruction but also serves as a key link between biological activity and

surface processes. Its universality across different environments provides a new perspective for understanding the evolution of the Earth's critical zone.

5 Conclusion

(1) The most dominant species on marble surfaces in the study area is *Myxosarcina* sp., followed by *Gomphosphaeria* sp., *Asterocapsa* sp.1, *Gloeocapsa* sp.1, and *Scytonema* sp.1. These aerobic cyanobacteria prefer calcareous environments, are drought-tolerant, slow-growing, and extremely resilient.

(2) The biological population composition on marble surfaces facing different directions of the Altar of Prayer for Good Harvests in the Temple of Heaven varies due to differences in sunlight exposure. The east-facing side, warm and humid, mainly hosts small filamentous and spherical cyanobacteria such as *Scytonema* sp.2 and *Gomphosphaeria* sp. The west-facing side, hot and humid, primarily features *Scytonema* sp.1 and mosses, with *Scytonema* sp.1 being small filamentous cyanobacteria. The north-facing side, cold and humid, mainly supports spherical cyanobacteria like *Myxosarcina* sp. and *Gomphosphaeria* sp. The south-facing side, hot and dry, primarily hosts small or large filamentous cyanobacteria such as *Scytonema* sp.1 and *Nostoc* sp.. The observed weathering intensity in different directions is: south > west > east > north, which is entirely consistent with the varying degrees of weathering reflected by the cloud dragon heads in each direction. This indicates that the visual analysis method based on the relative volume and relative volume percentage of species, as determined by microscopic observation and statistical analysis, is scientifically valid.

(3) Rock surface biological communities in the study area display various colors, with gray-black being the most common, followed by gray-white, black, brown, and brown-black. Gray-black communities are mainly composed of *Myxosarcina* sp. and *Gomphosphaeria* sp.

(4) Rock surface biological communities in the study area exhibit different morphologies, including membranous, hairy, carpet-like, leathery, shell-like, and powder layers. Different morphologies correspond to different population compositions.

(5) In addition to sunlight exposure, the growth of aerial organism on the rock surfaces in the study area is also controlled by macro-hydrological dynamics and micro-surface topography. On a macro scale, in areas with low flow during heavy rain, the biofilm is sparse, and the

bioweathering effect is weak. In areas with high-flow areas during heavy rain, "ink bands" rich in cyanobacteria form, leading to strong bioweathering. On a micro scale, the microtopographic features of the rock regulate local hydrological conditions, determining the colonization patterns of the organisms: On uneven or heterogeneous marble surfaces, aerial organism communities are distributed in patches, leading to the formation of solution pores, cavities, and pits; On marble surfaces with linear patterns or heterogeneous textures with joint lines, aerial organism communities are distributed in linear patterns, leading to the formation of solution marks, grooves, and channels. On flat and homogeneous marble surfaces, aerial organism communities are distributed in a planar pattern, leading to the formation of weathering layers or spalling layers. The thicker exopolysaccharide (EPS) sheath of aerial cyanobacteria can undergo contraction and expansion, thereby accelerating the disintegration of rock particles on the surface of rocks. Preventing or reducing the growth of aerial organism is key to slowing down the bioweathering process of the marble at the Altar of Prayer for Good Harvests in the Temple of Heaven.

**Author contributions**

YT completed all the work on the paper, including sampling, photography, experimental data analysis, charting, drawing, and writing the paper, among other tasks.

**Competing interests**

The author has declared that there are no competing interests.

**Acknowledgement**

This study was supported by National Science Foundation of China (Grant No. 40872197) and the Development Fund of China University of Geosciences (Beijing) (Grant No. F02114).

**References**

Beijing Institute of Ancient Architecture.: Research and Application of Stone Structure Protection in Ancient Buildings in Beijing. Beijing: China Literature and History Press. 1-330, 2018.

C. Gaylarde, C.: Influence of Environment on Microbial Colonization of Historic Stone Buildings

with Emphasis on Cyanobacteria. Heritage. 3. 1469-1482. https://doi.org/10.3390/heritage3040081, 2020

Checcucci, A, Borruso, L, Petrocchi, D, Perito, B.: Diversity and metabolic profile of the microbial communities inhabiting the darkened white marble of Florence Cathedral. International Biodeterioration & Biodegradation, 171- . https://doi.org/10.1016/j.ibiod.2022.105420, 2022.

Danin, A., Caneva, G.: Deterioration of limestone walls in Jerusalem and marble monuments in Rome caused by cyanobacteria and cyanophilous lichens. International Biodeterioration, 26(6): 397-417, https://doi.org/10.1016/0265-3036(90)90004-Q, 1990

Desikachary, T. V.: Cyanophyta. Indian Council of Agricultural Research. New Delhi.1~669. https://doi.org/10.1086/403350, 1959

Fott, B. (Translated by Luo,d.).: Phycology. Shanghai: Shanghai Science and Technology Press. 11-396, 1980.

Geitler, L.: Cyanophyceae. In L.Rabenhorst'S Kryptogamen-Flora, Band 14. Leipzig, Germany: Akademische Verlagsgesellsehaft m.b.H..1~1194, 1932.

Gioventù, E., Lorenzi, P. F., Villa, F., Sorlini, C., Rizzi, M., Cagnini, A., Griffo, A., Cappitelli, F.: Comparing the bioremoval of black crusts on colored artistic lithotypes of the Cathedral of Florence with chemical and laser treatment. International Biodeterioration & Biodegradation, 65(6): 832-839, https://doi.org/10.1016/j.ibiod.2011.06.002, 2011

Golubić, S, Pietrini, A M, Ricci, S.: Euendolithic activity of the cyanobacterium Chroococcus lithophilus Erc. In biodeterioration of the Pyramid of Caius Cestius, Rome, Italy. International Biodeterioration & Biodegradation, 100: 7-16, https://doi.org/10.1016/j.ibiod.2015.01.019, 2015

Gorbushina, A. Lyalikova, N. Vlasov, D.Y. Khizhnyak, T.: Microbial communities on the monuments of Moscow and St. Petersburg: biodiversity and trophic relations. Microbiology, 71, 350-356, https://doi.org/10.1023/A:1015823232025, 2002

Guiamet, P., Crespo, M., Lavin, P., Ponce, B., Gaylarde, C., Saravia, S. G. D.: Biodeterioration of funeral sculptures in La Recoleta Cemetery, Buenos Aires, Argentina: Pre- and post-intervention studies. Colloids and Surfaces B: Biointerfaces, 101: 337-342, https://doi.org/10.1016/j.colsurfb.2012.06.025, 2013.

Guillitte, O., Dreesen, R: Laboratory chamber studies and petrographical analysis as bioreceptivity

assessment tools of building materials, Science of The Total Environment, Volume 167, Issues 1–3, 365-374, https://doi.org/10.1016/0048-9697(95)04596-S, 1995

He, H.: Study on the Weathering of Marble Jinshi Steles in Beijing Confucius Temple. Capital Museum Forum, (35): 226-231, 2021.

Hu, H., Wei, Y. (Editors).: Systematics, Classification, and Ecology of Freshwater Algae in China. Beijing: Science Press. 23-203, 2006.

Isola, D., Zucconi, L., Onofri, S., Caneva, G., Selbmann, L.: Extremotolerant rock inhabiting black fungi from Italian monumental sites. Fungal Diversity 76, 75–96. https://doi.org/10.1007/s13225-015-0342-9, 2016

Jung, P., Baumann, K., Emrich, D., Springer, A., Felde, V. J. M. N. L., Dultz, S., Baum, C., Frank, M., Büdel, B., Leinweber, P.: Lichens Bite the Dust – A Bioweathering Scenario in the Atacama Desert. iScience, 23, 101647. https://doi.org/10.1016/j.isci.2020.101647, 2020

Komarek, J., Anagnostidis, K.: Cyanoprokaryota 1. Teil: Chroococcales. Vol. 19(1), In: Ettl H., Gaertner G, Heynig, H. and Mollenhauer, D. (eds.), Suesswasserflora von Mitteleuropa, Gustav Fischer, Jena-Stuttgart-Luebeck:Ulm. 1-548. https://doi.org/10.2216/i0031-8884-38-6-544.1, 1998.

Komarek, J, Anagnostidis, K.: Cyanoprokaryota 2. Teil: Oscillatoriales. Vol. 19(2), In: Büdel B., Gärtner G, Krienitz, L. and Schagerl, M. (eds.), Suesswasserflora von Mitteleuropa. Heidelberg, Germany: Springer Spektrum. 1-759, 2005.

Komarek, J., Büdel, B., Gärtner, G. Süßwasserflora von Mitteleuropa, Bd. 19/3: Cyanoprokaryota: 3. Teil / 3rd part: Heterocytous Genera. Springer Spektrum, 2013

Korkanç, M, Savran, A.: Impact of the surface roughness of stones used in historical buildings on biodeterioration. Construction and Building Materials, 80: 279-294, https://doi.org/10.1016/j.conbuildmat.2015.01.073, 2015

Lefler, F.W., Berthold, D.E., Laughinghouse, H. D.: Cyanoseq: A database of cyanobacterial 16S rRNA gene sequences with curated taxonomy. J. Phycol., 59: 470-480, https://doi.org/10.1111/jpy.13335, 2023.

Leo, F., D., Antonelli, F., Pietrini, A., M., Ricci, S., Urzì, C.: Study of the euendolithic activity of black meristematic fungi isolated from a marble statue in the Quirinale Palace's Gardens in Rome, Italy. Facies, 65,18, https://doi.org/10.1007/s10347-019-0564-5, 2019

Li, J.: Research on mechanical properties evaluation and deterioration mechanism of heritage rock in different environment. Master's Thesis. Beijing: Beijing University of Civil Engineering and Architecture. 1-72. https://link.cnki.net/doi/10.26943/d.cnki.gbjzc.2023.000478, 2023.

Liu, J.: Experimental study of thermal effects on Physical-mechanical properties of Beijing dolomitic marble. Master's Thesis. Beijing: China University of Geosciences (Beijing). 1-78. https://link.cnki.net/doi/10.27493/d.cnki.gzdzy.2020.001911, 2020.

Lombardozzi, V., Castrignanò, T., Antonio, M. D., Municchia, A C, Caneva, G.: An interactive database for an ecological analysis of stone biopitting. International Biodeterioration & Biodegradation, 73: 8-15, https://doi.org/10.1016/j.ibiod.2012.04.016, 2012

Lü, J., Wei, J.: Contribution of Dashiwo Marble in Fangshan, Beijing to the Foundation of the Forbidden City and Stone Sutras of Yunju Temple. Fossil, (03): 68-73, 2020.

Macedo, M F , Miller, A Z, Dionísio, A, Saiz-Jimenez, C: Biodiversity of cyanobacteria and green algae on monuments in the Mediterranean Basin: An overview. Microbiology, 155(Pt 11): 3476-3490. https://doi.org/10.1099/mic.0.032508-0, 2009

Marvasi, M., Cavalieri, D., Mastromei, G., Casaccia, A., Perito, B.: Omics technologies for an in-depth investigation of biodeterioration of cultural heritage. Int. Biodeterior. Biodegrad., 144, https://doi.org/104736, 10.1016/j.ibiod.2019.104736, 2019

Marvasi, M., Donnarumma, F., Frandi, A., Mastromei, G., Sterflinger, K., Tiano, P., Perito, B.: Black microcolonial fungi as deteriogens of two famous marble statues in Florence, Italy, International Biodeterioration & Biodegradation, Volume 68, 36-44, https://doi.org/10.1016/j.ibiod.2011.10.011, 2012

Mascalchi, M., Osticioli, I., Cuzman, O. A., Mugnaini, S., Giamello, M., Siano, S.: Laser removal of biofilm from Carrara marble using 532 nm: The first validation study, Measurement, V. 130, 255-263, https://doi.org/10.1016/j.measurement.2018.08.012 , 2018

Miller, A., Dionísio, A., Macedo, M. F.: Primary bioreceptivity: A comparative study of different Portuguese lithotypes. International Biodeterioration & Biodegradation, 57(2): 136-142. https://doi.org/10.1016/j.ibiod.2006.01.003, 2006.

Miller, A.Z. Sanmartín, P., Pereira-Pardo, L., Dionísio,    A., Saiz-Jimenez, C., Macedo, M.F., Prieto, B.: Bioreceptivity of building stones: A review, Science of The Total Environment, Volume 426, 1-12, https://doi.org/10.1016/j.scitotenv.2012.03.026, 2012

Monte, M Del, Sabbioni, C.: Chemical and bioweathering of an historical building: Reggio Emilia Cathedral. Science of The Total Environment, 50: 165-182, https://doi.org/10.1016/0048-9697(86)90358-X., 1986

Moropoulou, A, Bisbikou, K, Torfs, K, Van Grieken, R, Zezza, F, Macri, F.: Origin and growth of weathering crusts on ancient marbles in industrial atmosphere. Atmospheric Environment, 32(6): 967-982, https://doi.org/10.1016/S1352-2310(97)00129-5, 1998

Pinna, D, Galeotti, M, Perito, B, Daly, G, Salvadori, B.: In situ long-term monitoring of recolonization by fungi and lichens after innovative and traditional conservative treatments of archaeological stones in Fiesole (Italy), International Biodeterioration & Biodegradation, Volume 132, 49-58, https://doi.org/10.1016/j.ibiod.2018.05.003, 2018

Pinna, D.: Coping with Biological Growth on Stone Heritage Objects: Methods, Products, Applications, and Perspectives (1st ed.). Apple Academic Press. https://doi.org/10.1201/9781315365510, 2017

Praderio, G., Schiraldi, A., Sorlini, C., Stassi, A., Zanardini, E.: Microbiological and calorimetric investigations on degraded marbles from the Cà d'Oro facade (Venice). Thermochimica Acta, 227: 205-213. https://doi.org/10.1016/0040-6031(93)80263-A, 1993.

Qu, S.: The research on the weathering mechanism and weathering degree evaluation system of marble relics in Beijing. Master's Thesis. Beijing: Beijing University of Chemical Technology. 1-140, 2018.

Santo, A., P., Agostini, B., Cuzman, O., A., Michelozzi, M., Salvatici, T., Perito, B.: Essential oils to contrast biodeterioration of the external marble of Florence Cathedral, Science of The Total Environment,V. 877, https://doi.org/10.1016/j.scitotenv.2023.162913,2023,

Scheerer, S., Ortega-Morales, O., & Gaylarde, C.: Microbial deterioration of stone monuments—an updated overview. Advances in Applied Microbiology, 66, 97–139, https://doi.org/10.1016/S0065-2164(08)00805-8, 2009

Tian, Y., Zhang, J., Song, L., Bao, H.: A study on aerial algae communities on the surface of carbonate rock of the Yunnan stone forest. Carsologica Sinica, (03): 39-47, 2003.

Tian, Y., Zhang, J., Song, L., Bao, H.: A Study on Aerial Cyanophyta (Cyanobacteria) on the Surface of Carbonate Rock in Yunnan Stone Forest, Yunnan Province, China. Acta Ecologica Sinica, (11): 1793-1802+2020-2022, 2002.

Tian, Y., Zhang, J., Song, L., Bao, H.: The role of aerial algae in the formation of the landscape of the Yunnan Stone Forest, Yunnan Province, China. Science in China, Series D: Earth Sciences, 47(9): 846-864., 2004.

Timoncini, A., Costantini, F., Bernardi, E., Martini, C., Mugnai, F., Mancuso, F. P., Sassoni, E., Ospitali, F., & Chiavari, C.: Insight on bacteria communities in outdoor bronze and marble artefacts in a changing environment. Science of the Total Environment, 850, https://doi.org/10.1016/j.scitotenv.2022.157804, 2022

Trovão, J., Portugal, A.: The impact of stone position and location on the microbiome of a marble statue. The Microbe, 2, 100040. https://doi.org/10.1016/j.microb.2024.100040, 2024

Venturi,S., Tassi, F.,Cabassi, J. ,Gioli,B. ,Baronti, S.,Vaselli, O.,Caponi,C. ,Vagnoli,C. Picchi, G.,Zaldei, A.,Magi, F.,Miglietta, F. ,Capecchiacci, F. :Seasonal and diurnal variations of greenhouse gases in Florence (Italy): Inferring sources and sinks from carbon isotopic ratios, Science of The Total Environment, Volume 698, https://doi.org/10.1016/j.scitotenv.2019.134245,2020.

Wang, F, Fu, Y, Li, D, Huang, Y, Wei, S.: Study on the mechanism of the black crust formation on the ancient marble sculptures and the effect of pollution in Beijing area. Heliyon, 8(9): e10442, 2022

Wang, S.: The characteristic analysis of surface deterioration and mechanism study on West Yellow Temple Stone heritage. Master's Thesis. Beijing: China University of Geosciences (Beijing). 1-57, 2010.

Warscheid, T., Braams, J.: Biodeterioration of stone: a review. International Biodeterioration & Biodegradation, 46(4): 343-368, https://doi.org/10.1016/S0964-8305(00)00109-8, 2000

Wu, M., Liu, J.: Fangshan Dashiwo and Stone Quarrying for Ming Dynasty Palaces and Tombs in Beijing - Also on Stone Usage in Beijing's Imperial Construction Through Dynasties. Proceedings of the Palace Museum (First Volume). 253-262, 1996.

Wu, Y., Zhang, B., Zhang, J., Zhai, K., Luo, L.: Weathering Characteristics of White Marble Relics Around the Hall of Supreme Harmony (Taihe Dian) in the Forbidden City. KSCE Journal of Civil Engineering, 27(2): 794-804, https://link.cnki.net/doi/10.1007/s12205-022-1108-z 2023.

Yang, X.: Study on Weathering mechanism of Beijing Marble. Master's Thesis. Beijing: China

910          University of Geosciences (Beijing): 1-92, 2016.

911     Ye, J., Zhang, Z.: Correlation Study of Physical and Mechanical Parameters of Beijing Marble.

912          Journal          of          Engineering          Geology,          27          (3):          532-538.

913          https://link.cnki.net/doi/10.13544/j.cnki.jeg.2018-102, 2019.

914     Zhang, G.: Research on the weathering mechanism and Protection technology of spalling disease of

915          Marble relics in Beijing. Master's Thesis. Beijing: Beijing University of Chemical Technology.

916          1-77. https://link.cnki.net/doi/10.26939/d.cnki.gbhgu.2022.000801, 2022.

917     Zhang, T., Li, D., Zhang, Z.: Damage categories and deterioration mechanism of stone cultural relics

918          of white marble in Beijing. Geotechnical Investigation & Surveying, 44 (11): 7-13, 2016.

919     Zhang, Z., Yang, X., Ye, F., et al.: Microscopic characteristics of petrography and discussion on

920          weathering mechanism of Fangshan marble in Beijing. Journal of Engineering Geology, 23

921          (02): 279-286. https://link.cnki.net/doi/10.13544/j.cnki.jeg.2015.02.013, 2015.

922     Zheng, L., Li, K., Wang, J., Li, L., Wang, Y., Wang, M.: Investigations on the surface deterioration

923          process and mechanisms of white marble. Construction and Building Materials, 472: 140844,

924          https://link.cnki.net/doi/10.1016/j.conbuildmat.2025.140844, 2025

925     Zhu, H.: Freshwater Algae in China (Volume 2, Orders Chroococcales). Beijing: Science Press. 1-

926          105, 1991.

927

928

929

930